

QCD two-loop corrections for hadronic single top-quark production in the t -channel

M. Assadsolimani, P. Kant, B. Tausk, P. Uwer

Humboldt-Universität zu Berlin, Institut für Physik,
Newtonstraße 15, D-12489 Berlin, Germany

Abstract:

In this article we discuss the calculation of single top-quark production in the t -channel at two-loop order in QCD. In particular we present the decomposition of the amplitude according to its spin and colour structure and present complete results for the two-loop amplitudes in terms of master integrals. For the vertex corrections compact analytic expressions are given. The box contributions are implemented in a publicly available C program.

1. Introduction

In hadronic collisions top quarks are dominantly produced in pairs through the flavour conserving strong interaction. The charged currents of the weak interaction allow to produce top-quarks or anti-quarks also singly. Since the threshold for single top-quark production is half that of top-quark pair production, the weak coupling is partially compensated by phase space effects, and the larger parton fluxes such, that for LHC operating at 13 TeV the cross section for single top-quark production is roughly one third of the top-quark pair cross section. Despite these significant event rates, single top-quark production is experimentally challenging due to the complicated experimental signature and the sizeable backgrounds. To cope with these difficulties sophisticated experimental techniques like for example the matrix element method and methods making use of neural networks have been developed at the Tevatron and at the LHC [1–4]. Using these techniques, very precise measurements will be possible at the LHC running at 13 TeV. Physics wise single top-quark production is highly interesting since it allows a precise test of the top-quark weak couplings. In particular, single top-quark production offers a unique source of highly polarized top quarks. Furthermore the Cabibbo-Kobayashi-Maskawa (CKM) matrix element V_{tb} is directly accessible without further assumptions. In addition, single top-quark production can be used to constrain the bottom quark distribution inside the proton.

Depending on the momentum of the W boson involved in the charged current interaction, three different contributions to single top-quark production can be distinguished: the t -channel contribution for space-like momentum, the s -channel contribution for time-like momentum and the tW channel for on-shell production of a W boson in association with the top quark. At both colliders, Tevatron and LHC, the t -channel gives the largest contribution to the cross section. The second important channel at the LHC is tW production. This contribution is suppressed at the Tevatron due to the limited energy of the collider. The s -channel contributes about 30-40% to the cross section at the Tevatron while it is small at the LHC. The situation

	LHC 13 TeV				Tevatron	
	σ_t^{LO}	$\sigma_{\bar{t}}^{\text{LO}}$	σ_t^{NLO}	$\sigma_{\bar{t}}^{\text{NLO}}$	$\sigma_{t,\bar{t}}^{\text{LO}}$	$\sigma_{t,\bar{t}}^{\text{NLO}}$
t	135	79.8	$137^{+4.0}_{-2.3}^{+1.0}_{-0.9}$	$82.1^{+2.5}_{-1.3}^{+0.6}_{-0.8}$	1.03	$0.998^{+0.025}_{-0.022}^{+0.029}_{-0.032}$
s	4.27	2.63	$6.25^{+0.06}_{+0.09}^{+0.12}_{-0.09}$	$3.97^{+0.04}_{+0.05}^{+0.08}_{-0.07}$	0.28	$0.442^{+0.023}_{+0.025}^{+0.015}_{-0.011}$
tW	29.1	29.1	$29.3^{+1.0}_{-1.3}^{+0.7}_{-0.8}$	$29.2^{+1.0}_{-1.3}^{+0.7}_{-0.8}$	0.069	$0.070^{+0.002}_{-0.001}^{+0.008}_{-0.009}$

Table 1: Cross sections for single top-quark production in pb, for $m_t = 173.3$ GeV, $\mu_R = \mu_f = m_t$ and the MSTW2008lo/nlo PDF set, obtained using the Hathor program [5]. The sub- and superscripts denote the uncertainty due to scale variation and PDF uncertainties.

is summarized in Tab. 1 where also predictions at next-to-leading order (NLO) accuracy are given. The NLO corrections have been calculated for the different channels in Refs. [6–14]. The corrections to the t -channel are very small. However, the small size of the corrections is due to a significant cancellation between individual contributions. Furthermore, only the vertex corrections contribute to the cross section. The box-type corrections to the amplitude vanish when interfered with the Born amplitude. In particular, no colour exchange between the two incoming quark lines is possible in the t -channel. As a consequence it is conceivable that the small size of the NLO corrections is accidental and significant contributions at NNLO could appear when colour exchange between the two quark lines becomes possible. In particular, differential distributions which are crucial to test the $V - A$ structure of the weak interaction and the polarization of the top-quark imprinted by the production mechanism, may be affected significantly once the NNLO QCD corrections are taken into account. Very recently partial results for single top-quark production at NNLO accuracy have been presented for the t -channel in Ref. [15]. The analysis is restricted to the vertex corrections and the related real corrections. The corrections to the inclusive cross sections are at the level of one per cent and thus small from a phenomenological point of view. However, compared to the NLO corrections, they amount to about 50% and are thus much larger than one would naively expect — indicating that the full NNLO corrections may indeed give important corrections. The full NNLO corrections require the evaluation of a variety of different contributions: two-loop amplitudes interfered with the Born amplitude, corrections due to one-loop amplitudes squared, one-loop corrections to the real emission processes, and finally double real emission

processes. For most of the contributions established methods for their evaluation exist. In some cases even public tools are available to perform the required calculations. As far as the two-loop amplitudes are concerned the situation is more involved. In principle, techniques exist for the reduction of two-loop tensor integrals to a small set of master integrals. However, in practice this reduction and the evaluation of the master integrals is highly non-trivial and has been solved in the past only on a case by case basis. Depending on the number of invariants and masses the complexity of the reduction increases. In this article we present the complete reduction of the two-loop amplitudes for the t -channel. Results for the s -channel can be obtained through crossing or by adapting the reduction presented here. In section 2 we discuss the decomposition of the two-loop amplitudes according to the spin and colour structure. We also comment on our treatment of γ_5 in d space-time dimensions. In section 3 we present some details about the integral reduction. In section 4 we present the complete 2-loop amplitude in terms of master integrals further decomposed according to colour and spin structure. For the vertex corrections compact analytic results are given. As far as the double box contributions are concerned we briefly discuss their numerical evaluation using an implementation in C which can be obtained on demand. Due to their length it is not useful to present analytic expressions here. We close with a short conclusion in section 5.

2. Theoretical setup

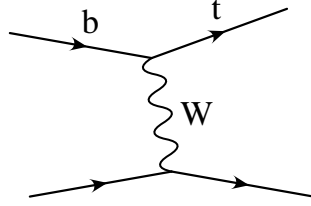


Figure 1: Born diagram for t -channel production of a single top quark.

In this section we briefly describe the theoretical setup used to organise the calculation of the two-loop amplitudes for single top-quark production in the t -channel. To fix our conventions, we consider the partonic process

$$u(k_u) + b(k_b) \rightarrow t(k_t) + d(k_d), \quad (1)$$

treating all quarks — with the exception of the top quark — as massless. We define two Mandelstam variables by

$$\hat{t} = (k_b - k_t)^2 = m_t^2 - 2k_b k_t, \quad \hat{s} = (k_u + k_b)^2 = 2k_u k_b. \quad (2)$$

At leading order in the electroweak coupling g_W , the amplitude for this process is expanded in the strong coupling constant $\alpha_s = \frac{g_s^2}{4\pi}$:

$$\mathcal{A} = g_W^2 V_{tb} V_{ud}^* \left(\mathcal{A}^{(0)} + \frac{\alpha_s}{4\pi} \mathcal{A}^{(1)} + \left(\frac{\alpha_s}{4\pi} \right)^2 \mathcal{A}^{(2)} + \dots \right). \quad (3)$$

The Born contribution is given by

$$\mathcal{A}^{(0)} = \delta_{tb} \delta_{du} A_1^{(0)}, \quad (4)$$

with

$$A_1^{(0)} = \frac{1}{\hat{t} - m_W^2} \bar{u}(k_t) \gamma_\mu \frac{1}{2} (1 - \gamma_5) u(k_b) \bar{u}(k_d) \gamma^\mu \frac{1}{2} (1 - \gamma_5) u(k_u). \quad (5)$$

The electroweak coupling can be expressed in terms of the electric charge e of a positron and the sine of the Weinberg mixing angle ϑ_W through

$$g_W = \frac{e}{\sqrt{2} \sin(\vartheta_W)}. \quad (6)$$

Working in leading order in the electroweak coupling, the renormalization scheme of the electroweak parameters is not fixed. For phenomenological applications one may use the on-shell scheme in which the weak mixing angle can be calculated from the mass of the Z -boson (m_Z) and the mass of the W -boson (m_W) using:

$$\cos^2(\vartheta_W) = \frac{m_W^2}{m_Z^2}. \quad (7)$$

The matrix elements of the Cabibbo-Kobayashi-Maskawa matrix, which expresses the eigenstates of the weak interaction in terms of the mass eigenstates, are denoted by V_{ij} . Since the Born amplitude is a purely electroweak process, no colour exchange between the two quark lines is possible. This is reflected in the colour structure $\delta_{tb} \delta_{du}$ where t, b, \dots describe the colour indices of the respective quarks and δ denotes the Kronecker delta. However, when higher order QCD corrections are included, colour exchange between the two quark lines does become possible. In two-loop approximation about 70 Feynman diagrams contribute to the transition matrix element — not counting self-energy corrections and counter term diagrams. Sample diagrams are shown in Fig. 2. As we shall see in the following, many diagrams do not contribute to the cross section at NNLO accuracy. The colour decomposition of the two-loop amplitude reads:

$$\mathcal{A}^{(2)} = \delta_{tb} \delta_{du} A_1^{(2)} + \left(\delta_{tu} \delta_{db} - \frac{1}{N} \delta_{tb} \delta_{du} \right) A_2^{(2)}, \quad (8)$$

where N denotes the number of colours. We work with the general $SU(N)$ gauge group, to make the colour structure more explicit. The QCD case is obtained by setting $N = 3$. Using the Fierz identity

$$(T^a)_{ij} (T^a)_{kl} = T_r \left(\delta_{il} \delta_{kj} - \frac{1}{N} \delta_{ij} \delta_{kl} \right), \quad (9)$$

where T^a ($a = 1 \dots N^2 - 1$) are the generators of $SU(N)$ in the fundamental representation (we use the normalization $\text{tr}(T^a T^b) = T_r \delta_{ab}$, with $T_r = \frac{1}{2}$), it follows that all Feynman diagrams where only one gluon is exchanged between the two quark lines contribute only to $A_2^{(2)}$. Owing to the simple colour structure of the Born amplitude, the contribution $A_2^{(2)}$ does not contribute to the cross section at order α_s^2 . In particular, Feynman diagrams involving a

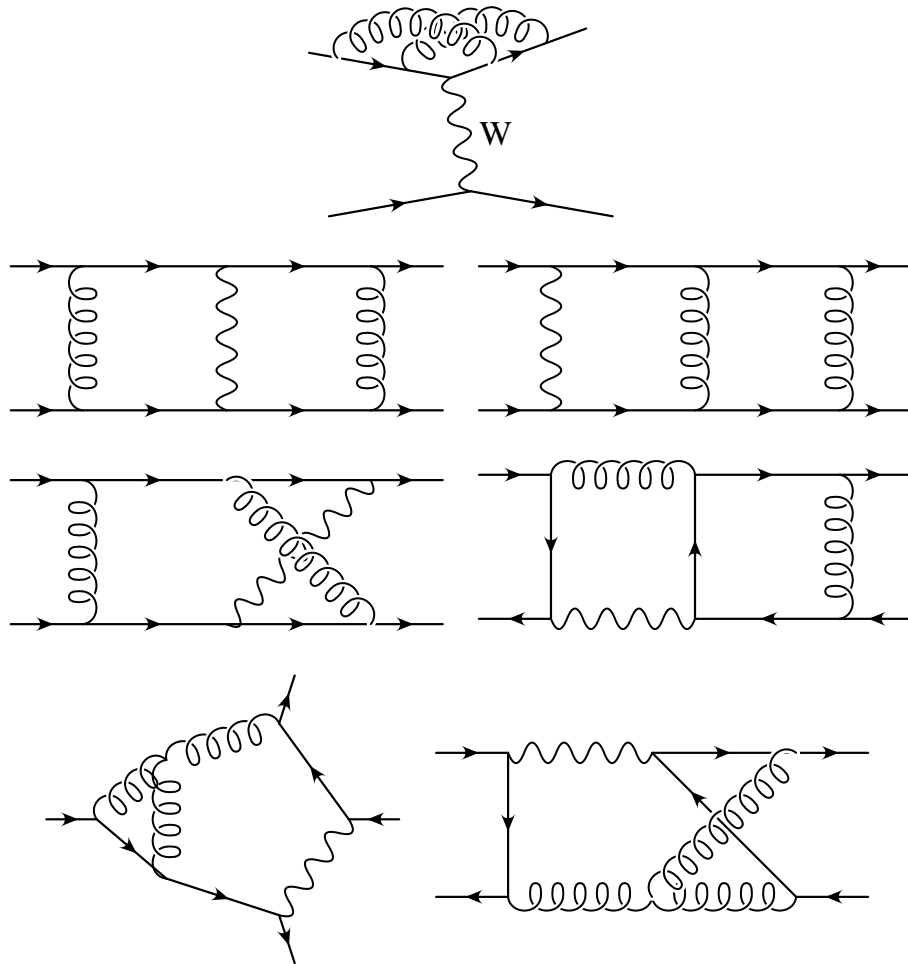


Figure 2: Sample diagrams for single top-quark production at two-loop order.

pentagon sub-loop (for an example see the last row in Fig. 2) vanish after interference with the Born amplitude. This is similar to the one-loop corrections, where box-topologies do not contribute to the cross section in order α_s . (Note however, that the one-loop box diagrams squared start to contribute to the cross section at order α_s^2 .) Using the colour decomposition as shown in Eq. (4) and Eq. (8) we obtain for the interference of the two-loop amplitude with the Born amplitude:

$$\sum_{\text{color}} \mathcal{A}^{(0)*} \mathcal{A}^{(2)} = N^2 A_1^{(0)*} A_1^{(2)}. \quad (10)$$

Making the N dependence of $A_1^{(2)}$ explicit it is possible to decompose $A_1^{(2)}$ further into leading- and sub-leading colour contributions:

$$A_1^{(2)} = (N^2 - 1) \left(A_{1,LC}^{(2)} + \frac{1}{N} T_r(B_h + n_l B_l) + \frac{1}{N^2} A_{1,SC}^{(2)} \right) \quad (11)$$

The contributions B_h , B_l are due to self-energy insertions in the one-loop topologies. B_l is due to massless quarks (n_l counts the number of massless quark flavours), while B_h is due to a top-quark loop in the gluon propagator. Interfering the full two-loop amplitude with the Born amplitude we thus obtain

$$\sum_{\text{color}} \mathcal{A}^{(0)*} \mathcal{A}^{(2)} = N^2 (N^2 - 1) \left(A_1^{(0)*} A_{1,LC}^{(2)} + \frac{T_r}{N} A_1^{(0)*} (B_h + n_l B_l) + \frac{1}{N^2} A_1^{(0)*} A_{1,SC}^{(2)} \right). \quad (12)$$

The surviving diagrams can be classified into the following different groups:

1. Gluonic self-energy corrections due to closed quark loops inserted into one-loop topologies, contributing to B_h and B_l ,
2. A single diagram, consisting of two one-loop vertex corrections to the two weak vertices (first diagram in Fig. 3), contributing to $A_{1,LC}^{(2)}$ and $A_{1,SC}^{(2)}$,
3. Two-loop vertex corrections, contributing to $A_{1,LC}^{(2)}$ and $A_{1,SC}^{(2)}$,
4. Planar and non-planar double-box topologies, contributing to $A_{1,SC}^{(2)}$.

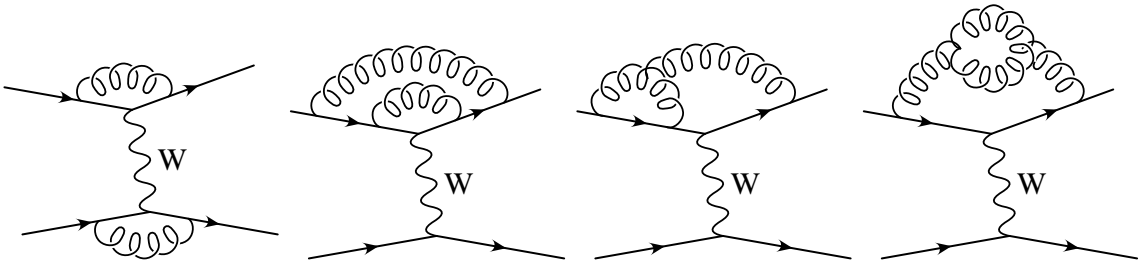


Figure 3: Sample topologies contributing to $A_{1,LC}^{(2)}$.

In Fig. 3 sample topologies contributing to $A_{1,LC}$ are shown. The Feynman diagrams involving the three gluon vertex contribute only to $A_{1,LC}^{(2)}$ while the other topologies contribute to $A_{1,LC}^{(2)}$ and $A_{1,SC}^{(2)}$.

Let us now discuss the spin structure of the amplitude, which we compute in Feynman gauge, using dimensional regularization to regularize ultraviolet and infrared divergences. A typical term in the calculation consists of spinors and gamma matrices, contracted with tensor integrals of the form

$$I_n(d, \mathbf{v}_1, \dots, \mathbf{v}_n) [\ell_1^{\alpha_1} \dots \ell_1^{\alpha_{N_1}} \ell_2^{\beta_1} \dots \ell_2^{\beta_{N_2}}] = \int d^d \ell_1 d^d \ell_2 \frac{\ell_1^{\alpha_1} \dots \ell_1^{\alpha_{N_1}} \ell_2^{\beta_1} \dots \ell_2^{\beta_{N_2}}}{D_1^{v_1} \dots D_n^{v_n}}, \quad (13)$$

with scalar propagator denominators D_i which are functions of the loop momenta ℓ_1, ℓ_2 and of the external momenta k_j . The propagators appear with powers v_i which may be different from one. The tensor integrals in eq. (13) can be reduced to a basis of tensors constructed from metric tensors and the external momenta k_j

$$I_n(d, \mathbf{v}_1, \dots, \mathbf{v}_n) [\ell_1^{\alpha_1} \dots \ell_1^{\alpha_{N_1}} \ell_2^{\beta_1} \dots \ell_2^{\beta_{N_2}}] = \sum_i C_i T_i^{\alpha_1 \dots \alpha_{N_1} \beta_1 \dots \beta_{N_2}}, \quad (14)$$

with scalar coefficients C_i . Next, the basic tensors $T_i^{\alpha_1 \dots \alpha_{N_1} \beta_1 \dots \beta_{N_2}}$ are contracted with the spinors and gamma matrices, and the resulting expressions are simplified by applying rules of the Dirac algebra.

At this point we need to specify how γ_5 is treated in d -dimensional space-time. It is well known that γ_5 is an intrinsically four-dimensional object and cannot be generalized in a smooth way to d dimensions. Different prescriptions to deal with γ_5 can be found in the literature (see for example Refs. [16–21]). In the 't Hooft-Veltman scheme or variants thereof an explicit definition of γ_5 in d dimensions is given. For example in the 't Hooft-Veltman scheme one uses

$$\gamma_5 = i\gamma_0\gamma_1\gamma_2\gamma_3. \quad (15)$$

In d dimensions we now have

$$\{\gamma_5, \gamma_\mu\} = \gamma_5\gamma_\mu + \gamma_\mu\gamma_5 = 0 \text{ for } \mu = 0, \dots, 3 \quad (16)$$

and

$$[\gamma_5, \gamma_\mu] = 0, \text{ for } \mu \neq 0, \dots, 3. \quad (17)$$

In general, the naive application of such a scheme violates Ward identities involving the axial-vector current, since the derivation of the same typically relies on formal manipulations using an anti-commuting γ_5 . These Ward identities have to be restored using additional counter terms (see for example Ref. [22]) unless they correspond to observable effects related to axial-vector current anomalies. In contrast, a prescription which ensures $\{\gamma_5, \gamma_\mu\} = 0$, guarantees that axial-vector Ward identities are reproduced. However, using anti-commutativity together with the cyclicity of the trace operation it is trivial to show that

$$\text{Tr}(\gamma_5\gamma_\alpha\gamma_\beta\gamma_\gamma\gamma_\delta) = 0 \quad (18)$$

for $d \neq 4$. A way out is to choose the scheme as proposed in Refs. [20, 21] where the cyclicity of the trace is given up. In fact as pointed out in Ref. [23] the method proposed in Ref. [18] can also be understood as a modification of the trace operation. An anti-commuting γ_5 obviously fails to reproduce the Adler-Bell-Jackiw anomaly. Since in the present calculation no anomalous contribution arises we use $\{\gamma_5, \gamma_\mu\} = 0$.

Using an anti-commuting γ_5 in d dimensions, and taking into account that only terms with an odd number of Dirac matrices along the massless quark line connecting the external d and u quarks can appear, we find that the spinor structures in any of the two-loop diagrams can be reduced to a linear combination of the following 11 basic structures:

$$\begin{aligned}
S_1 &= \bar{u}(k_t) \gamma_7 u(k_b) \times \bar{u}(k_d) \gamma_6 \not{k}_t u(k_u) \\
S_2 &= \bar{u}(k_t) \gamma_6 \not{k}_u u(k_b) \times \bar{u}(k_d) \gamma_6 \not{k}_t u(k_u) \\
S_3 &= \bar{u}(k_t) \gamma_6 \gamma_{\mu_1} u(k_b) \times \bar{u}(k_d) \gamma_6 \gamma_{\mu_1} u(k_u) \\
S_4 &= \bar{u}(k_t) \gamma_7 \gamma_{\mu_1} \not{k}_u u(k_b) \times \bar{u}(k_d) \gamma_6 \gamma_{\mu_1} u(k_u) \\
S_5 &= \bar{u}(k_t) \gamma_7 \gamma_{\mu_1} \gamma_{\mu_2} u(k_b) \times \bar{u}(k_d) \gamma_6 \gamma_{\mu_1} \gamma_{\mu_2} \not{k}_t u(k_u) \\
S_6 &= \bar{u}(k_t) \gamma_6 \gamma_{\mu_1} \gamma_{\mu_2} \not{k}_u u(k_b) \times \bar{u}(k_d) \gamma_6 \gamma_{\mu_1} \gamma_{\mu_2} \not{k}_t u(k_u) \\
S_7 &= \bar{u}(k_t) \gamma_6 \gamma_{\mu_1} \gamma_{\mu_2} \gamma_{\mu_3} u(k_b) \times \bar{u}(k_d) \gamma_6 \gamma_{\mu_1} \gamma_{\mu_2} \gamma_{\mu_3} u(k_u) \\
S_8 &= \bar{u}(k_t) \gamma_7 \gamma_{\mu_1} \gamma_{\mu_2} \gamma_{\mu_3} \not{k}_u u(k_b) \times \bar{u}(k_d) \gamma_6 \gamma_{\mu_1} \gamma_{\mu_2} \gamma_{\mu_3} u(k_u) \\
S_9 &= \bar{u}(k_t) \gamma_7 \gamma_{\mu_1} \gamma_{\mu_2} \gamma_{\mu_3} \gamma_{\mu_4} u(k_b) \times \bar{u}(k_d) \gamma_6 \gamma_{\mu_1} \gamma_{\mu_2} \gamma_{\mu_3} \gamma_{\mu_4} \not{k}_t u(k_u) \\
S_{10} &= \bar{u}(k_t) \gamma_6 \gamma_{\mu_1} \gamma_{\mu_2} \gamma_{\mu_3} \gamma_{\mu_4} \not{k}_u u(k_b) \times \bar{u}(k_d) \gamma_6 \gamma_{\mu_1} \gamma_{\mu_2} \gamma_{\mu_3} \gamma_{\mu_4} \not{k}_t u(k_u) \\
S_{11} &= \bar{u}(k_t) \gamma_6 \gamma_{\mu_1} \gamma_{\mu_2} \gamma_{\mu_3} \gamma_{\mu_4} \gamma_{\mu_5} u(k_b) \times \bar{u}(k_d) \gamma_6 \gamma_{\mu_1} \gamma_{\mu_2} \gamma_{\mu_3} \gamma_{\mu_4} \gamma_{\mu_5} u(k_u), \tag{19}
\end{aligned}$$

where $\gamma_6 = 1 + \gamma_5$ and $\gamma_7 = 1 - \gamma_5$. Here, we have not applied any four-dimensional Fierz identities, which could be used to simplify the structures further in four dimensions. We conclude that each of the colour-stripped amplitudes B_h , B_l , $A_{1,LC}^{(2)}$ and $A_{1,SC}^{(2)}$ has a decomposition in spinor structures of the form

$$A^{(2)} = \sum_{i=1}^{11} f_i S_i. \tag{20}$$

Note that the general form of this decomposition does not depend on the actual values of the scalar coefficients C_i in Eq. (14).

We have used two different methods to calculate the scalar coefficients. The first method, developed by Tarasov [24, 25], relates these coefficients to scalar integrals with increased powers of the propagators v_i and in higher space-time dimensions. Our implementation of this method closely follows the approach of Ref. [26], where all formulae required for two-loop applications can be found. Here, we limit ourselves to a very brief summary. Introducing a Schwinger parameter x_i for each of the propagators D_i , the denominator of Eq. (13) is written as

$$\frac{1}{D_1^{v_1} \dots D_n^{v_n}} = \int \mathcal{D}x \exp \left(\sum_{i=1}^n x_i D_i \right), \tag{21}$$

where

$$\mathcal{D}x = \prod_{i=1}^n \frac{(-1)^{v_i} x_i^{v_i-1}}{\Gamma(v_i)} dx_i. \quad (22)$$

In terms of the loop momenta, the exponent has the form

$$\sum_{i=1}^n x_i D_i = a \ell_1^2 + b \ell_2^2 + 2c (\ell_1 \cdot \ell_2) + 2(d \cdot \ell_1) + 2(e \cdot \ell_2) + f, \quad (23)$$

with coefficients a, b, c, d^μ, e^μ, f that are linear in the Schwinger parameters. The loop momentum integrations are now Gaussian and can be performed straightforwardly. In the case of a scalar integral, one finds that

$$I_n(d, v_1, \dots, v_n)[1] \propto \int \mathcal{D}x \frac{\exp(Q/\mathcal{P})}{\mathcal{P}^{d/2}}, \quad (24)$$

where \mathcal{P} and Q are polynomials in the Schwinger parameters, defined by

$$\mathcal{P} = ab - c^2 \quad (25)$$

$$Q = -ae^2 - bd^2 + 2c(d \cdot e) + f\mathcal{P}. \quad (26)$$

For tensor integrals, similar expressions are obtained, with additional polynomials in the Schwinger parameters, divided by powers of \mathcal{P} , multiplying the integrand in Eq. (24). From the form of Eq. (22), one sees that any additional factor of x_i in the numerator of Eq. (24) can be interpreted as a shift $v_i \rightarrow v_i + 1$ in the power of the corresponding propagator. Similarly, any additional factor of $1/\mathcal{P}$ is equivalent to a shift of the space-time dimension $d \rightarrow d + 2$. The final result is that each scalar coefficient C_i in Eq. (14) is expressed as a sum of scalar integrals $I(d + 2m, v_1 + \delta_1, \dots, v_n + \delta_n)[1]$.

In the second method of determining the scalar coefficients, both sides of Eq. (14) are contracted with tensors T_i . In this way, a system of linear equations is obtained relating the C_i to integrals with numerators containing scalar polynomials in the loop momenta. The number of independent coefficients to be determined can be reduced by exploiting the symmetry properties of the tensor integrals in Eq. (13) with respect to permutations of the Lorentz indices [27]. Both methods lead to identical results in the end, once all scalar integrals involved have been expressed in terms of a set of independent master integrals. However, the scalar integrals appearing in the intermediate steps of the two methods are different.

In addition to these two methods, we have also used a third approach, where we do not use the scalar coefficients C_i explicitly, but, instead, directly project out the functions f_i in the spinor decomposition of Eq. (20). This turns out to be the most efficient method, especially for the most complicated diagrams, which are the double boxes. The projection works by contracting the amplitude with the conjugate spinor structure \mathcal{S}_j^* and taking the trace of the two spinor chains:

$$\sum_i \text{Tr}[\mathcal{S}_j^* \mathcal{S}_i] f_i = \text{Tr}[\mathcal{S}_j^* A^{(2)}]. \quad (27)$$

We define a matrix of contractions

$$\mathcal{M}_{ji} = \text{Tr}[S_j^* S_i], \quad (28)$$

whose entries are polynomials in d , \hat{s} , \hat{t} , and m_t . The functions f_i are now obtained from the inverse matrix:

$$f_i = (\mathcal{M}^{-1})_{ij} \text{Tr}[S_j^* A^{(2)}]. \quad (29)$$

Having proven the general decomposition shown in Eq. (20) with the spinor structures shown in Eq. (19) we can simplify the calculation of the f_i by setting γ_5 to zero. Evidently this has to be done in the evaluation of \mathcal{M} and in the evaluation of $\text{Tr}[S_j^* A^{(2)}]$. This is possible because in a theory with purely vector couplings we would get precisely the same spinor structures as given in Eq. (20) but with γ_5 set to zero everywhere. In other words the scalar functions f_i multiplying the 11 spinor structures do not care whether we have purely vector coupling or $(V - A)$ coupling as long as we use an anti-commuting γ_5 . Note that this does not mean that both theories give the same results for the two-loop amplitude interfered with the Born amplitude. When we calculate the interference term we need to keep the γ_5 in the spin-structures. A similar method has been used recently in Ref. [15] where it has been argued that γ_5 can be always anti-commuted to the bracketing spinors where one can absorb γ_5 into the spinor for a specific helicity. (In principle one could also keep γ_5 in the aforementioned steps using a concrete prescription to evaluate the trace, i.e. the method from Ref. [21].) The trace operation in $\text{Tr}[S_j^* S_i]$ allows to get rid of all spinor structures and to express the results in terms of two-loop integrals, where the loop momenta appear only in scalar products with external momenta or again loop momenta. It is thus possible to cancel some of them with corresponding factors in the denominator. To proceed, we need to express these integrals in terms of master integrals. This reduction will be discussed in the next section.

3. Reduction to master integrals

Depending on how the two-loop amplitude is projected onto the eleven spin structures, the starting point for the reduction of the tensor integrals to a small set of scalar master integrals is different. Using the dimension-shifting method, one ends up with scalar integrals with raised powers of the propagators and in higher space-time dimensions. Inspecting Fig. 2 and Fig. 3, we observe that the most complicated tensor integrals have rank 4, leading to scalar integrals in $d + 8$ dimensions with the powers of the propagators increased in total by eight units. On the other hand, using the projection method of Eq. (29) to determine the scalar functions f_i multiplying the different spinor structures, we obtain scalar integrals with irreducible scalar products in the numerator. In this case, the most complicated integrals are double-box integrals with 4 irreducible scalar products in the numerator. Employing integration-by-parts (IBP) identities [28, 29], relations between different integrals can be established. These relations can then be used to reduce the appearing integrals to the master integrals. An algorithmic solution of the reduction procedure has been given with the Laporta algorithm [30], in which an overconstrained system of equations is set up, which is then used to express all integrals

in terms of a few integrals. Different implementations of the Laporta algorithm are publicly available as computer code [31–36]. As the main working horse for the reduction described in this article, we used the program `Reduze 2` [35] written in C++. In addition, we used a private version of the program `Crusher` made available to us by P. Marquard [37].

3.1. Reduction of vertex diagrams

For the reduction of the vertex diagrams we used both methods to reduce the amplitude to the spinor structures. The highest tensor integrals are of rank four. As mentioned before, using the dimension-shifting method leads thus to scalar integrals with the powers of the propagators raised by up to 8 units. In addition, the dimension of the space-time is shifted to $d + 8$. Reducing these integrals using the IBP equations requires two steps. In the first step, integrals with raised powers of the propagators defined for arbitrary but fixed space-time dimension are reduced to master integrals. In a second step, the master integrals in $d + 2m$ dimensions ($m = 1, \dots, 4$) are transformed back to master integrals in d dimensions, using the dimension shift operator \mathcal{P} (see Eq. (24)) and the reduction table derived in the first step. Using instead Eq. (29) to reduce the amplitude to the spin structures S_i , we apply the Laporta algorithm to integrals involving irreducible scalar products. Since all the integrals stay in d dimensions a dimension shift is not required. For the vertex corrections, we have applied both methods and found complete agreement between them.

As a further check on our programs, we have recalculated the two-loop QCD corrections to the heavy quark vector and axial vector form factors, applying both the dimension-shifting method and the projection method. After substituting ϵ -expansions for the master integrals from Ref. [38], we found complete agreement with the results available in the literature [39, 40].

3.2. Reduction of the double-box diagrams

The reduction of the double-box diagrams involves 9 different topologies, three planar ones and six non-planar topologies. For each topology two different diagrams exist. Since the two diagrams belonging to the same topology are connected, it is sufficient to determine the reduction tables only once for each of the nine topologies.

The reduction of the double-box topologies is significantly more complicated than the vertex corrections. The increased complexity is due to the larger number of propagators and to the simple fact that the double-box diagrams involve more scales. In the double-box topologies the W -boson mass appears in the two-loop integrals. In addition, the double-box topologies involve \hat{s} and \hat{t} while the two-loop form factors depend only on \hat{t} . Applying the dimension-shifting method, we were not able to generate all the required reduction tables, using the aforementioned programs. On the other hand, for the simpler double-box topologies, we were able to reduce also the highest tensor ranks appearing in the calculation when applying the

projectors of Eq. (29). However, even in this case, we were not able to fully reduce the most complicated double-box topologies. As mentioned before, the increased complexity of the double-box topologies as compared to the vertex corrections, is a direct consequence of the large number of independent variables. In the reduction rational functions in the five variables $\hat{s}, \hat{t}, m_t, m_W$ and d are generated. The manipulation of these rational functions, in combination with the related increase of expression size, leads to much longer run time and also increased memory consumption. Having said this, the direction to simplify the reduction is obvious: One needs to reduce the number of independent variables. Using one variable out of $\hat{s}, \hat{t}, m_t, m_W$ to define the mass scale will reduce the number of independent variables by one. Expressing in addition the top-quark mass in terms of the W -boson mass (or vice versa), will further reduce the number of independent variables by one. In Ref. [41] the most precise measurements from the Tevatron experiments CDF and D0 and the LHC experiments ATLAS and CMS have been combined. The *world average* quoted in Ref. [41] reads

$$m_t = 173.34 \pm 0.27 \text{ (stat)} \pm 0.71 \text{ (syst)} \text{ GeV}/c^2. \quad (30)$$

Using in addition the world average for m_W as produced by the particle data group [42]

$$m_W = 80.385 \pm 0.015 \text{ GeV}/c^2, \quad (31)$$

we can set to very good approximation

$$m_t^2 \approx \frac{14}{3} m_W^2, \quad (32)$$

which is equivalent to

$$m_t \approx 173.65 \text{ GeV}/c^2. \quad (33)$$

This value for the top-quark mass is compatible with the aforementioned world average and deviates less than 2 per mille from the central value quoted in Eq. (30). Since single top-quark production depends very weakly on the top-quark mass around the nominal value, the uncertainty introduced by the aforementioned approximation is completely negligible. (Using this approximation in leading order would lead to effects at the per mille level. For more details we refer to Ref. [5] where the mass dependence of single top-quark production has been studied in detail.) Choosing Eq. (32) to reduce the number of independent variables, leads indeed to an enormous simplification of the reduction procedure. In addition, we also fine tuned, for the most complicated topologies, the seed generation in the Laporta algorithm. Using these two techniques, we were able to reduce all the double-box integrals to master integrals. In cases where the reduction was feasible for arbitrary values of m_W and m_t , the two approaches agreed, after specializing the general results to the specific case $m_t^2 = \frac{14}{3} m_W^2$. In addition, we observed a dramatic reduction in the size of the final expressions, when setting $m_t^2 = \frac{14}{3} m_W^2$.

4. Results

In this section, we present analytic results for $A_{1,LC}^{(2)}$, B_h and B_l . The vertex contributions to $A_{1,SC}^{(2)}$ are given in appendix A. The master integrals entering the corrections to the W - t -

b vertex are known in the literature from studies of the form factors describing the decay $b \rightarrow u + W^*$, with $m_u = 0$, $m_b \neq 0$ [43–49]. For master integrals entering the corrections to the light quark vertex, see also Ref. [50]. In the results shown below, the master integrals are kept as symbols, and also the full d dependence is kept. In choosing the basis for the master integrals, we follow Refs. [43–45]. The definitions of the master integrals are given in appendix B. For the presentation of the results, it is convenient to introduce rescaled invariants

$$t = \frac{\hat{t}}{m_t^2}, \quad s = \frac{\hat{s}}{m_t^2}. \quad (34)$$

Note, that the vertex corrections only depend on the W -boson mass through the W -boson propagator. All vertex contributions thus have a universal factor

$$\frac{1}{\hat{t} - m_W^2}.$$

Furthermore, the form factors only depend on \hat{t} . The entire \hat{s} dependence is thus hidden in the spinor structures \mathcal{S}_1 and \mathcal{S}_3 . For the contribution of the light quark loops we obtain:

$$\begin{aligned} 2(\hat{t} - m_W^2) \times B_l = & \frac{\text{MI301pu1}}{16(d-4)(d-1)(2d-7)(t-1)}(d-2) \\ & \times \left[\mathcal{S}_1 \left(16(d^3 - 11d^2 + 39d - 44) \right) - \mathcal{S}_3 \left((3d-8)(d(t-3) - 6t + 10) \right) \right] \\ & - \frac{\text{MI401}}{2(d-4)(d-1)(3d-8)} \\ & \times \left[\mathcal{S}_3 \left((d-2)(3d^3 - 31d^2 + 110d - 128) \right) \right] \\ & - \frac{\text{MI402p}}{2(d-4)(d-1)(3d-8)(t-1)} \\ & \times \left[\mathcal{S}_1 \left(8(d-4)(d-2)(d^2 - 7d + 11) \right) \right. \\ & \left. + \mathcal{S}_3 \left((d-2)(3d^3 - 31d^2 + 110d - 128)t - (d-4)(d-2)(3d^2 - 22d + 36) \right) \right]. \end{aligned} \quad (35)$$

The contribution due to closed top-quark loops reads:

$$\begin{aligned} 2(\hat{t} - m_W^2) \times B_h = & \frac{(\text{MI101p})^2}{16(d-7)^2(d-6)(d-5)^2(d-4)(d-3)(d-1)(3d-8)(t-1)^3 t} \\ & \times \left[4\mathcal{S}_1(d-7)^2(d-2) \left(-(d-2)(11d^6 - 270d^5 + 2670d^4 \right. \right. \\ & \left. \left. - 13592d^3 + 37443d^2 - 52686d + 29424)t^3 \right. \right. \\ & \left. \left. + 2(17d^7 - 466d^6 + 5294d^5 - 32312d^4 + 114473d^3 - 235626d^2 + 261228d - 120408)t^2 \right) \right] \end{aligned}$$

$$\begin{aligned}
& + (17d^7 - 424d^6 + 4414d^5 - 24884d^4 + 82377d^3 - 161352d^2 + 174804d - 81552)t \Big) \\
& + \mathcal{S}_3(d-2) \Big(-2(d-7)(d-6)^2(d-4)(d-3)(d-2)(d-1)(3d-8)t^5 \\
& + (7d^8 - 256d^7 + 4017d^6 - 35257d^5 + 189540d^4 \\
& - 641323d^3 + 1342244d^2 - 1604508d + 847776)t^4 \\
& + (24d^9 - 999d^8 + 18280d^7 - 192775d^6 + 1288447d^5 - 5644750d^4 \\
& + 16162933d^3 - 29085772d^2 + 29772324d - 13172352)t^3 \\
& + (209d^8 - 7096d^7 + 103443d^6 - 843419d^5 + 4192720d^4 \\
& - 12956457d^3 + 24167772d^2 - 24676020d + 10419168)t^2 \\
& - (d-3)(24d^8 - 781d^7 + 10663d^6 - 79156d^5 + 347337d^4 \\
& - 926691d^3 + 1529312d^2 - 1610140d + 963072)t \\
& + 32(d-7)^2(d-6)(d-5)(d-4)(d-3)^2(d-1) \Big) \Big] \\
& + \frac{\text{MI101p} \times \text{MI201}}{(d-7)(d-5)(d-4)(d-1)(3d-8)t} \\
& \times \Big[\mathcal{S}_3 \Big((d^2 - 5d + 6)(3d^3 - 29d^2 + 74d - 48)t \\
& - 2(d^2 - 5d + 6)(3d^4 - 51d^3 + 334d^2 - 946d + 936) \Big) \Big] \\
& + \frac{\text{MI101p} \times \text{MI201p}}{(d-7)(d-5)(d-4)(d-1)(3d-8)(t-1)^3} \\
& \times \Big[\mathcal{S}_3 \Big((d-6)(d-3)(d-2)(d-1)(3d-8)t^3 \\
& - 2(d-3)(d-2)(3d^4 - 48d^3 + 305d^2 - 872d + 888)t^2 \\
& + (d-5)(d-3)(d-2)(6d^3 - 81d^2 + 338d - 416)t \Big) \\
& + \mathcal{S}_1 \Big(-8(d-7)(d-4)(d-3)(d-2)(d^2 - 12d + 21)t \Big) \Big] \\
& + \frac{\text{MI303p}}{8(d-7)(d-6)(d-4)(d-1)(t-1)^3} \\
& \times \Big[\mathcal{S}_3 \Big(-(3d-8)(2d^3 - 27d^2 + 93d - 58)t^3 \\
& + (4d^4 - 49d^3 + 133d^2 + 62d - 320)t^2 \\
& - (3d-8)(2d^3 - 21d^2 + 55d + 2)t \\
& + (d-3)(8d^3 - 103d^2 + 386d - 256) \Big) \\
& + 4\mathcal{S}_1(d-7) \Big((d^4 - 14d^3 + 59d^2 - 82d + 16)t^2 \\
& - 2(d-2)(3d^3 - 30d^2 + 73d - 26)t \\
& - (3d^4 - 30d^3 + 89d^2 - 98d + 56) \Big) \Big]
\end{aligned}$$

$$\begin{aligned}
& + \frac{\text{MI406t}}{4(d-7)(d-5)(d-1)(3d-8)t} \\
& \quad \times \left[\mathcal{S}_3 \left((d-6)(d-1)(3d-10)(3d-8)t^2 \right. \right. \\
& \quad \left. \left. - 2(d-4)(3d^4 - 55d^3 + 334d^2 - 674d + 300)t + 32(d-7)(d-5)(d-3)(d-1) \right) \right] \\
& + \frac{\text{MI407p}}{4(d-7)(d-5)(d-1)(3d-8)(t-1)^3} \\
& \quad \times \left[\mathcal{S}_1 \left(8(d-7)(d-4)(d^3 - 2d^2 + d - 10)t^2 \right. \right. \\
& \quad + 16(d-7)(3d^4 - 34d^3 + 119d^2 - 138d + 20)t \\
& \quad + 8(d-7)(d-4)(d^3 - 2d^2 + d - 10) \Big) \\
& \quad + \mathcal{S}_3 \left((d-6)(d-1)(3d-10)(3d-8)t^4 \right. \\
& \quad - 2(d-5)(3d^4 - 34d^3 + 150d^2 - 236d + 48)t^3 \\
& \quad + 2(d-4)(9d^4 - 116d^3 + 491d^2 - 630d - 40)t^2 \\
& \quad - 2(9d^5 - 155d^4 + 972d^3 - 2582d^2 + 2324d + 320)t \\
& \quad \left. \left. + (d-5)(2d^2 - 17d + 32)(3d^2 - 16d + 4) \right) \right] \\
& + \frac{\text{MI407t}}{2(d-7)(d-5)(d-1)(3d-8)} \\
& \quad \times \left[\mathcal{S}_3 \left((d-6)(d-1)(3d-8)t^2 + 2(5d^3 - 45d^2 + 64d + 68)t - 8(d^3 - 13d^2 + 84d - 164) \right) \right] \\
& + \frac{\text{MI408p}}{2(d-7)(d-5)(d-1)(3d-8)(t-1)} \\
& \quad \times \left[\mathcal{S}_1 \left(8(d-7)(d^3 - 8d^2 + 23d - 26) + 8(d-7)t(d^3 - 8d^2 + 23d - 26) \right) \right. \\
& \quad + \mathcal{S}_3 \left((d-6)(d-1)(3d-8)t^3 + (-5d^3 + 55d^2 - 242d + 376)t^2 \right. \\
& \quad \left. \left. - (3d-8)(d^2 - 3d - 2)t + (d-5)(d-4)(5d-22) \right) \right]. \tag{36}
\end{aligned}$$

The leading colour contribution is given by:

$$\begin{aligned}
& (\hat{t} - m_W^2) \times A_{1,LC}^{(2)} = \\
& \frac{(\text{MI101p})^2}{32(d-5)(d-4)^2(d-3)^2(t-1)^3t}(d-2) \\
& \quad \times \left[2\mathcal{S}_1(d-4) \left(-(d-2)(2d^5 - 35d^4 + 244d^3 - 779d^2 + 980d - 144)t^3 \right. \right. \\
& \quad + (8d^6 - 157d^5 + 1140d^4 - 3993d^3 + 6782d^2 - 3984d - 1184)t^2 \\
& \quad - (6d^6 - 117d^5 + 950d^4 - 3821d^3 + 7394d^2 - 5300d - 380)t \\
& \quad \left. \left. + (d-3)^2(d^3 - 14d^2 + 60d - 84) \right) \right]
\end{aligned}$$

$$\begin{aligned}
& +S_3 \left(-(d-2)(5d^4 - 53d^3 + 182d^2 - 186d - 48)t^4 \right. \\
& \quad + (4d^7 - 89d^6 + 825d^5 - 4036d^4 + 10626d^3 - 12526d^2 - 588d + 10112)t^3 \\
& \quad - (8d^7 - 185d^6 + 1747d^5 - 8434d^4 + 20774d^3 - 19174d^2 - 13504d + 28112)t^2 \\
& \quad + (4d^7 - 95d^6 + 903d^5 - 4228d^4 + 9254d^3 - 3874d^2 - 17524d + 21120)t \\
& \quad \left. - (d-4)(d-3)^2(d^3 - 14d^2 + 60d - 84) \right) \Big] \\
& - \frac{\text{MI101p} \times \text{MI201}}{4(d-4)^2(d-3)(t-1)} \times (d^3 - 9d^2 + 30d - 32) \times [S_1(d^2 - 9d + 20) + S_3(d+t-3)] \\
& + \frac{\text{MI101p} \times \text{MI201p}}{8(d-5)(d-4)^2(d-3)(t-1)^3(t+1)} \\
& \times \left[2S_1(d-4) \left((d-2)(6d^4 + 6d^3 - 599d^2 + 2965d - 4194)t^3 \right. \right. \\
& \quad - (2d^6 - 132d^5 + 1624d^4 - 8801d^3 + 25103d^2 - 37864d + 24316)t^2 \\
& \quad + (50d^5 - 618d^4 + 2823d^3 - 5771d^2 + 4952d - 1140)t \\
& \quad \left. + (2d^6 - 44d^5 + 424d^4 - 2301d^3 + 7367d^2 - 12988d + 9676) \right) \\
& + S_3 \left(-(d-2)(d^5 - 33d^4 + 361d^3 - 1811d^2 + 4330d - 4040)t^4 \right. \\
& \quad + (-2d^7 + 58d^6 - 723d^5 + 5167d^4 - 23052d^3 + 63656d^2 - 99048d + 65856)t^3 \\
& \quad + (2d^7 - 68d^6 + 1001d^5 - 8085d^4 + 38330d^3 - 106292d^2 + 159488d - 99936)t^2 \\
& \quad + (2d^7 - 42d^6 + 307d^5 - 815d^4 - 548d^3 + 6520d^2 - 9560d + 2496)t \\
& \quad \left. - (d-4)(2d^6 - 45d^5 + 440d^4 - 2400d^3 + 7663d^2 - 13416d + 9916) \right) \Big] \\
& + \frac{(\text{MI201})^2}{4(d-4)^2} \times [S_3(d^2 - 7d + 16)^2] \\
& + \frac{\text{MI201} \times \text{MI201p}}{4(d-4)^2(t-1)} \times (d^2 - 7d + 16) \\
& \times \left[2S_1(d-5)(d-4) + S_3((d^2 - 7d + 16)t - (d-5)(d-4)) \right] \\
& + \frac{(\text{MI201p})^2}{4(d-4)^2(d-2)(t-1)^2} \\
& \times \left[2S_1(d-5)(d-4) \left((d-2)(d^2 - 7d + 20)t - (d-4)^2(d-3) \right) \right. \\
& \quad + S_3 \left((d-5)(d-3)(d-4)^3 - 2(d-5)(d^3 - 9d^2 + 31d - 36)t(d-4) \right. \\
& \quad \left. \left. + (d-2)(d^2 - 7d + 16)^2t^2 \right) \right] \\
& - \frac{\text{MI301}}{2(d-4)^3(d-3)t} \times S_3(3d-8)(d^5 - 18d^4 + 138d^3 - 552d^2 + 1144d - 980) \\
& + \frac{\text{MI301p}}{48(d-4)^2(d-3)(d-2)(3d-14)(3d-10)(t-1)^4t(t+1)} (3d-8)
\end{aligned}$$

$$\begin{aligned}
& \times \left[2S_1(d-4) \left(-3(d-2)(39d^5 - 168d^4 - 2953d^3 + 26640d^2 - 78364d + 79264)t^5 \right. \right. \\
& \quad - (1413d^6 - 27981d^5 + 234094d^4 - 1060948d^3 + 2745592d^2 - 3833952d + 2244096)t^4 \\
& \quad + 2(1206d^6 - 21423d^5 + 162301d^4 - 676348d^3 + 1640716d^2 - 2192784d + 1253568)t^3 \\
& \quad + 4(459d^6 - 7374d^5 + 47544d^4 - 157328d^3 + 283267d^2 - 268548d + 110124)t^2 \\
& \quad - (135d^6 - 3516d^5 + 39101d^4 - 229022d^3 + 734948d^2 - 1221192d + 821280)t \\
& \quad \left. \left. + (10-3d)^2(d-3)(d^3 - 14d^2 + 60d - 84) \right) \right] \\
& + S_3 \left(3(d-2)(3d-10)(3d^5 - 82d^4 + 825d^3 - 3946d^2 + 9128d - 8272)t^6 \right. \\
& \quad - (279d^7 - 7464d^6 + 87645d^5 - 581978d^4 + 2342908d^3 \\
& \quad - 5677752d^2 + 7621632d - 4349568)t^5 \\
& \quad + (837d^7 - 22503d^6 + 264520d^5 - 1748672d^4 + 6969480d^3 \\
& \quad - 16643600d^2 + 21946528d - 12284544)t^4 \\
& \quad - 2(387d^7 - 11778d^6 + 147097d^5 - 987170d^4 + 3867090d^3 \\
& \quad - 8873800d^2 + 11068952d - 5798304)t^3 \\
& \quad + (9d^7 - 2208d^6 + 36717d^5 - 247402d^4 + 816056d^3 \\
& \quad - 1258312d^2 + 540464d + 376704)t^2 \\
& \quad + (189d^7 - 5676d^6 + 71951d^5 - 498558d^4 + 2039584d^3 \\
& \quad - 4928840d^2 + 6519088d - 3642816)t \\
& \quad \left. \left. - (10-3d)^2(d-4)(d-3)(d^3 - 14d^2 + 60d - 84) \right) \right] \\
& + \frac{\text{MI301pu1}}{32(d-4)^2(d-3)(d-2)(d-1)(2d-7)(t-1)^3t} \\
& \times \left[2S_1(d-4) \left(-(d-2)(d^6 + 440d^5 - 6429d^4 + 35932d^3 - 95824d^2 + 119592d - 53472)t^3 \right. \right. \\
& \quad - (529d^7 - 9252d^6 + 70159d^5 - 299288d^4 + 772684d^3 - 1195216d^2 + 1007616d \\
& \quad - 346752)t^2 \\
& \quad - (d-3)(199d^6 - 1941d^5 + 4754d^4 + 9760d^3 - 63060d^2 + 97640d - 47232)t \\
& \quad \left. \left. + (d-3)(d-1)(3d-10)(3d-8)(d^3 - 14d^2 + 60d - 84) \right) \right] \\
& + S_3(3d-8) \left(-(d-2)(20d^5 - 311d^4 + 1903d^3 - 5618d^2 + 7740d - 3704)t^4 \right. \\
& \quad - (31d^7 - 704d^6 + 7086d^5 - 40145d^4 + 135102d^3 - 263900d^2 + 269960d - 107328)t^3 \\
& \quad + (59d^7 - 1512d^6 + 16118d^5 - 92351d^4 + 305548d^3 - 578716d^2 + 572296d - 221328)t^2 \\
& \quad - (d-4)(25d^6 - 652d^5 + 5982d^4 - 26367d^3 + 60042d^2 - 66876d + 27832)t \\
& \quad \left. \left. - (d-4)(d-3)(d-1)(3d-10)(d^3 - 14d^2 + 60d - 84) \right) \right]
\end{aligned}$$

$$\begin{aligned}
& + \frac{\text{MI302p}}{48(d-4)^2(d-3)^2(d-2)(3d-14)(3d-10)(t-1)^4(t+1)} \\
& \times \left[2S_1(d-4) \left(-3(d-4)(d-2)(39d^5 - 168d^4 - 2953d^3 + 26640d^2 - 78364d + 79264)t^6 \right. \right. \\
& \quad - (774d^7 - 26721d^6 + 356317d^5 - 2478482d^4 + 9901244d^3 \\
& \quad - 22954024d^2 + 28764096d - 15080448)t^5 \\
& \quad + (10827d^7 - 223305d^6 + 1981624d^5 - 9871708d^4 + 30022960d^3 \\
& \quad - 56104608d^2 + 59923968d - 28266240)t^4 \\
& \quad + 2(4770d^7 - 91863d^6 + 740791d^5 - 3234600d^4 + 8241086d^3 \\
& \quad - 12240312d^2 + 9841128d - 3343104)t^3 \\
& \quad + (1377d^7 - 18996d^6 + 62875d^5 + 328634d^4 - 3249632d^3 \\
& \quad + 10583832d^2 - 16053648d + 9585216)t^2 \\
& \quad - (126d^7 - 3213d^6 + 36817d^5 - 240990d^4 + 954816d^3 - 2255336d^2 + 2907792d \\
& \quad - 1564800)t \\
& \quad \left. + (10-3d)^2(d-4)(d-3)(d^3 - 14d^2 + 60d - 84) \right) \\
& + S_3 \left(3(d-4)(d-2)(3d-10)(3d^5 - 82d^4 + 825d^3 - 3946d^2 + 9128d - 8272)t^7 \right. \\
& \quad - 2(99d^8 - 3687d^7 + 56907d^6 - 485332d^5 + 2527836d^4 - 8280296d^3 \\
& \quad + 16711104d^2 - 19033056d + 9376896)t^6 \\
& \quad + (1854d^8 - 54405d^7 + 718453d^6 - 5542690d^5 + 27121572d^4 - 85585512d^3 \\
& \quad + 169096992d^2 - 190429312d + 93318144)t^5 \\
& \quad + (-2205d^8 + 75537d^7 - 1089466d^6 + 8726684d^5 - 42714580d^4 + 131331008d^3 \\
& \quad - 248352496d^2 + 264603584d - 121790976)t^4 \\
& \quad + (-333d^8 + 3348d^7 + 13303d^6 - 329746d^5 + 1816836d^4 - 4238712d^3 \\
& \quad + 2610176d^2 + 5461120d - 7300608)t^3 \\
& \quad + 2(342d^8 - 12798d^7 + 192703d^6 - 1576044d^5 + 7786640d^4 - 24034128d^3 \\
& \quad + 45561040d^2 - 48743168d + 22627584)t^2 \\
& \quad + (d-4)(180d^7 - 4833d^6 + 55603d^5 - 354122d^4 + 1343364d^3 \\
& \quad - 3023192d^2 + 3720832d - 1922496)t \\
& \quad \left. - (10-3d)^2(d-4)^2(d-3)(d^3 - 14d^2 + 60d - 84) \right) \Big] \\
& + \frac{\text{MI401}}{4(d-4)^2(d-1)(3d-8)} \\
& \times \left[S_3(-3d^6 + 82d^5 - 819d^4 + 4030d^3 - 10344d^2 + 12824d - 5632) \right]
\end{aligned}$$

$$\begin{aligned}
& - \frac{\text{MI402p}}{(d-2)(d-1)(3d-8)8(d-4)^2(t-1)^3(t+1)} \\
& \times \left[2S_1(d-4) \left((d-2)(17d^5 - 353d^4 + 2572d^3 - 8428d^2 + 12232d - 5920)t^3 \right. \right. \\
& \quad + (-143d^6 + 2019d^5 - 12632d^4 + 43772d^3 - 85488d^2 + 85936d - 33344)t^2 \\
& \quad + (-17d^6 - 141d^5 + 3278d^4 - 18348d^3 + 46172d^2 - 54120d + 23296)t \\
& \quad \left. \left. + (-d^6 + 45d^5 - 524d^4 + 2740d^3 - 7268d^2 + 9368d - 4480) \right) \right. \\
& \quad + S_3(t-1) \left(2(d-2)(3d^6 - 82d^5 + 819d^4 - 4030d^3 + 10344d^2 - 12824d + 5632)t^3 \right. \\
& \quad + (-33d^7 + 779d^6 - 7936d^5 + 44060d^4 - 141224d^3 + 257488d^2 - 243552d + 90112)t^2 \\
& \quad + 2(d-4)(15d^6 - 356d^5 + 3033d^4 - 12592d^3 + 27374d^2 - 29524d + 12096)t \\
& \quad \left. \left. - (d-4)(3d^6 - 73d^5 + 684d^4 - 3212d^3 + 8004d^2 - 9912d + 4608) \right) \right] \\
& + \frac{\text{MI501p}}{8(d-3)(d-2)(t-1)^3t(t+1)} \\
& \times \left[S_1 \left(2(d-8)(d-4)(d-2)^2t^5 \right. \right. \\
& \quad - 2(d-2)(29d^3 + 72d^2 - 1600d + 3552)t^4 \\
& \quad - 4(183d^4 - 1880d^3 + 7594d^2 - 14890d + 11984)t^3 \\
& \quad - 4(97d^4 - 766d^3 + 1686d^2 - 94d - 2064)t^2 \\
& \quad + 2(13d^4 - 288d^3 + 1968d^2 - 5508d + 5552)t \\
& \quad \left. \left. - 2(d-4)(d^3 - 14d^2 + 60d - 84) \right) \right. \\
& \quad + S_3 \left(-(d-2)(3d^3 + 8d^2 - 148d + 336)t^5 \right. \\
& \quad + (-47d^4 + 650d^3 - 4092d^2 + 12436d - 13888)t^4 \\
& \quad + 2(43d^4 - 780d^3 + 5076d^2 - 14092d + 13984)t^3 \\
& \quad - 2(9d^4 - 292d^3 + 2076d^2 - 5400d + 4616)t^2 \\
& \quad + (-19d^4 + 346d^3 - 2188d^2 + 5904d - 5856)t \\
& \quad \left. \left. + (d-4)(d^3 - 14d^2 + 60d - 84) \right) \right] \\
& + \frac{\text{MI502p}}{2(d-4)^2(d-3)(d-2)t(t^2-1)}(2d-9) \\
& \times \left[2S_1(d-4) \left((d-2)(d^2 + 22d - 96)t^3 + 3(11d^3 - 74d^2 + 200d - 208)t^2 \right. \right. \\
& \quad \left. \left. + (15d^3 - 52d^2 - 40d + 180)t - (d^3 - 14d^2 + 60d - 84) \right) \right. \\
& \quad + S_3 \left(2(d-2)(2d^2 - 15d + 30)t^4 + (5d^4 - 74d^3 + 470d^2 - 1408d + 1544)t^3 \right. \\
& \quad \left. \left. - (9d^4 - 166d^3 + 1094d^2 - 3068d + 3064)t^2 + (d-2)(3d^3 - 72d^2 + 402d - 652)t \right) \right]
\end{aligned}$$

$$+ (d-4)(d^3 - 14d^2 + 60d - 84) \Big] . \quad (37)$$

The sub-leading colour contribution of the vertex corrections to $A_{1,SC}^{(2)}$ is given in appendix A. We have also obtained analytic expressions for the double-box diagrams. However, the expressions of several megabytes are too long to be presented here. Since in the end, the main interest is in the numerical evaluation of the corrections and not so much in the analytic structure, we have generated computer code written in C to evaluate the contributions from double-box topologies. In the functions f_i appearing in the decomposition of the amplitude according to its spin structure as shown in Eq. (20), we have expanded the coefficient of each master integral in $\epsilon = (4-d)/2$:

$$f_i = \sum_r \sum_{s=-5}^4 \epsilon^s f_{i,r,s} \text{MI}_r . \quad (38)$$

The index r labels the master integrals MI. While some of them are known in the literature, the most complicated double-box integrals are not yet known and need to be calculated in the future. Assuming that only $\frac{1}{\epsilon^4}$ poles occur in the master integrals MI_r , it is sufficient to keep terms up to fourth order in ϵ in the coefficients of the master integrals. Note that the reduction procedure itself can lead to spurious poles in ϵ . These poles require to calculate also positive powers in ϵ for the master integrals. Alternatively, one may consider to change the basis of master integrals, to avoid the spurious poles to some extent. As mentioned in the previous section, we have calculated the double-box contribution for a fixed ratio m_W^2/m_t^2 . Using again the rescaled invariants s and t the coefficients are rational functions in s and t only. As proof of concept we have calculated all coefficients $f_{i,r,s}$ introduced above. They are encoded in the aforementioned C library. We have checked that the numerical results obtained using the C library agree with the original mathematica code used to produce the expressions. In this comparison it turns out to be crucial to use extended (quadruple) floating point precision. We trace this back to the observation, that integer constants occurring in the numerical evaluation vary over many orders of magnitude. We note that it is straightforward to change the integral basis used in the numerical evaluation. This can be done by rerunning the code generation. The code for the coefficients as introduced in Eq. (38) can be obtained on demand. Using extended floating point precision in the evaluation of the coefficients $f_{i,r,s}$ leads to an increased runtime. We do not consider this as a major problem: First of all, for the integration of the virtual corrections, typically a small number of phase space points is usually sufficient. In the practical application, one may calculate the two-loop contribution as a two-dimensional grid in s and t , which is interpolated during the calculation. The calculation of the grid can be parallelized. Furthermore, most likely the computational effort of the complete NNLO calculation will be dominated by the evaluation of the real corrections, in particular the double unresolved contributions.

5. Conclusion

In this article we consider two-loop QCD corrections for single top-quark production in the t -channel. We have decomposed the two-loop amplitude according to its colour and spin structure. Using an anti-commuting γ_5 , eleven different spin structures occur in the most complicated contributions. To reduce the two-loop tensor integrals to master integrals, we used the publicly available program Reduze [34, 35]. Cross checks were obtained using a private version of the program Crusher made available to us by Peter Marquard. For the vertex corrections, analytic results are presented valid in arbitrary space-time dimensions and for arbitrary masses. Since for the vertex corrections all master integrals are known, the leading-colour contribution to the two-loop amplitude can be calculated numerically, using the results presented in this article. For the double-box contributions, we considered a fixed ratio $m_W^2/m_t^2 = 3/14$, to reduce the complexity of the calculation. Even for this special case where the number of independent variables is reduced, the results are too long to be presented in analytic form. To illustrate the feasibility of the calculation — once all the master integrals are known — we have created a C library, allowing the calculation of the double-box diagrams. This library is generated automatically from the analytic results and can be obtained on demand.

Acknowledgments

We would like to thank Michal Czakon, Thomas Gehrmann and Andrey Grozin for useful discussions. We are very grateful to Cedric Studerus and Andreas von Manteuffel for assistance with Reduze 2 [35], and to Peter Marquard for making Crusher [37] available to us. We would also like to thank Sophia Borowka for advice on the use of SecDec [51], and Guido Bell for sending us an electronic version of the master integrals of Refs. [43–45]. The Feynman diagrams in our calculation were generated by QGRAF [52] and processed further, in part, using FORM [53]. This work is supported by the Helmholtz alliance HA-101 “Physics at the Terascale” and by the Deutsche Forschungsgemeinschaft in the Sonderforschungsbereich/Transregio SFB/TR-9 “Computational Particle Physics” and through the DFG Research Training Group GRK 1504 “Mass, Spectrum, Symmetry”.

A. Vertex contribution to $A_{1,SC}^{(2)}$

The sub-leading colour contribution of the vertex diagrams is given by:

$$(\hat{t} - m_W^2) \times A_{1,SC}^{(2)} = \frac{(MI101p)^2}{\frac{1}{(24 - 7d + 8t - 2dt - 4t^2 + dt^2)}(d - 2)} \frac{128(-5 + d)^2(-4 + d)^2(-3 + d)^2(-7 + 2d)(-8 + 3d)(-1 + t)^4 t(1 + t)(6 - d - 10t + 3dt)}{1}$$

$$\begin{aligned}
& \times \left[4S_1(d-5) \left(8(d-5)(d-4)^3(d-3)(d-2)(2d-7)(3d-10)(3d-8)t^9 \right. \right. \\
& \quad + (d-4)(72d^{10} - 2496d^9 + 37217d^8 - 311525d^7 + 1592803d^6 - 5001809d^5 \\
& \quad + 8776242d^4 - 4594508d^3 - 12037976d^2 + 23649600d - 13143040)t^8 \\
& \quad - (d-4)(456d^{10} - 15620d^9 + 234269d^8 - 2024207d^7 + 11116257d^6 - 40224087d^5 \\
& \quad + 95689188d^4 - 143362844d^3 + 120093376d^2 - 37593696d - 6961152)t^7 \\
& \quad + (360d^{11} - 13908d^{10} + 239927d^9 - 2457445d^8 + 16681741d^7 - 78969673d^6 \\
& \quad + 265901534d^5 - 634846884d^4 + 1046959112d^3 - 1125115136d^2 + 698682368d \\
& \quad - 185163776)t^6 \\
& \quad + (1944d^{11} - 73292d^{10} + 1240123d^9 - 12446713d^8 + 82294307d^7 - 375547289d^6 \\
& \quad + 1202264680d^5 - 2683212260d^4 + 4050878208d^3 - 3874266752d^2 + 2044742144d \\
& \quad - 416348160)t^5 \\
& \quad - (2472d^{11} - 92700d^{10} + 1548463d^9 - 15221501d^8 + 97812709d^7 - 430679297d^6 \\
& \quad + 1320775118d^5 - 2800487420d^4 + 3968522792d^3 - 3481789664d^2 + 1592171520d \\
& \quad - 224776192)t^4 \\
& \quad - (984d^{11} - 36524d^{10} + 643215d^9 - 7036377d^8 + 52447151d^7 - 276033761d^6 \\
& \quad + 1035505520d^5 - 2746965908d^4 + 5021880176d^3 - 6000847008d^2 + 4203434880d \\
& \quad - 1302693888)t^3 \\
& \quad + (2040d^{11} - 76092d^{10} + 1298069d^9 - 13328407d^8 + 91238503d^7 - 435788819d^6 \\
& \quad + 1476990730d^5 - 3539359148d^4 + 5853548856d^3 - 6333491392d^2 + 4010948864d \\
& \quad - 1116893184)t^2 \\
& \quad - (d-4)(504d^{10} - 17308d^9 + 265247d^8 - 2379033d^7 + 13756739d^6 - 53254969d^5 \\
& \quad + 138719412d^4 - 237663604d^3 + 252395024d^2 - 145947456d + 32799744)t \\
& \quad \left. + 2(d-6)(d-4)(d-3)^2(2d-7)(3d-8)(7d-24)(d^3 - 14d^2 + 60d - 84) \right) \\
& + S_3 \left(4(d-4)^2(d-3)(d-2)(2d-7)(3d-10)(3d-8)(d^3 - 12d^2 + 47d - 64)t^{10} \right. \\
& \quad - (d-4)(39d^{10} - 758d^9 + 1014d^8 + 102890d^7 - 1365961d^6 + 8953268d^5 \\
& \quad - 35633348d^4 + 90116280d^3 - 142168064d^2 + 128061984d - 50426624)t^9 \\
& \quad - 2(144d^{12} - 5853d^{11} + 106233d^{10} - 1125913d^9 + 7614893d^8 - 33329432d^7 \\
& \quad + 87548326d^6 - 82676166d^5 - 292510688d^4 + 1319679832d^3 - 2429628320d^2 \\
& \quad + 2295716736d - 912044032)t^8 \\
& \quad + 2(624d^{12} - 25517d^{11} + 467011d^{10} - 5024149d^9 + 34985681d^8 - 162697988d^7 \\
& \quad + 495353856d^6 - 872953574d^5 + 326362560d^4 + 2340163592d^3 - 5851837696d^2 \\
& \quad \left. + 6135096256d - 2561895936)t^7 \right)
\end{aligned}$$

$$\begin{aligned}
& + 2(240d^{12} - 7771d^{11} + 110613d^{10} - 899449d^9 \\
& + 4465165d^8 - 12495678d^7 + 6198642d^6 + 106764150d^5 - 512877072d^4 \\
& + 1284522024d^3 - 1965748896d^2 + 1745927296d - 694160384)t^6 \\
& - 2(2448d^{12} - 98940d^{11} + 1793243d^{10} - 19164393d^9 + 133274773d^8 - 625172561d^7 \\
& + 1963191740d^6 - 3827692686d^5 + 3208111312d^4 + 4073077832d^3 - 14872218784d^2 \\
& + 16882063040d - 7277689344)t^5 \\
& + 2(1488d^{12} - 64421d^{11} + 1222387d^{10} - 13385791d^9 + 93186883d^8 - 424085370d^7 \\
& + 1218939742d^6 - 1806863846d^5 - 691010600d^4 + 9062809384d^3 - 18505002528d^2 \\
& + 17734922880d - 6934335488)t^4 \\
& + 2(1488d^{12} - 58931d^{11} + 1079209d^{10} - 12100551d^9 + 92514971d^8 - 507226248d^7 \\
& + 2037633608d^6 - 6011525698d^5 + 12838263664d^4 - 19186420904d^3 \\
& + 18825711552d^2 - 10702091712d + 2585400832)t^3 \\
& - 2(1584d^{12} - 66423d^{11} + 1264341d^{10} - 14414743d^9 + 109335375d^8 - 579143804d^7 \\
& + 2185485568d^6 - 5874474730d^5 + 11022458856d^4 - 13756521592d^3 + 10301462432d^2 \\
& - 3551784064d + 57738240)t^2 \\
& + (672d^{12} - 28945d^{11} + 560716d^{10} - 6433612d^9 + 48420964d^8 - 249708795d^7 \\
& + 892337088d^6 - 2169762400d^5 + 3360836360d^4 - 2662256912d^3 - 284884128d^2 \\
& + 2342032896d - 1353775104)t \\
& - 4(d-6)(d-5)(d-4)(d-3)^2(2d-7)(3d-8)(7d-24)(d^3-14d^2+60d-84)) \Big] \\
& + \frac{\text{MI101p} \times \text{MI201}}{4(d-4)^2(d-3)(t-1)}(-2+d) \times (16-7d+d^2) \\
& \times \left[\mathcal{S}_3(d+t-3) + \mathcal{S}_1(d^2-9d+20) \right] \\
& + \frac{\text{MI101p} \times \text{MI201p}}{32(d-5)(d-4)^2(d-3)(2d-7)(3d-8)(t-1)^4(t+1)(dt^2-4t^2-2dt+8t-7d+24)} \\
& \times \left[\mathcal{S}_3 \left((d-4)(d-2)(3d-8)(8d^6-193d^5+1958d^4-10665d^3+32936d^2-55008d \right. \right. \\
& \quad \left. \left. + 39152)t^7 \right. \right. \\
& + 2(24d^{10} - 877d^9 + 14654d^8 - 148051d^7 + 1003072d^6 - 4755828d^5 + 15922406d^4 \\
& - 36982364d^3 + 56718880d^2 - 51597952d + 21047296)t^6 \\
& + (-192d^{10} + 6650d^9 - 105855d^8 + 1025274d^7 - 6711491d^6 + 31010198d^5 \\
& - 102014060d^4 + 234445784d^3 - 357683136d^2 + 324984832d - 132818944)t^5 \\
& - 4(d-4)(36d^9 - 1143d^8 + 15875d^7 - 129159d^6 + 689474d^5 - 2531265d^4 \\
& + 6408378d^3 - 10727464d^2 + 10654464d - 4723456)t^4 \\
& \left. \left. + (768d^{10} - 27668d^9 + 457159d^8 - 4565336d^7 + 30487811d^6 - 141920362d^5 \right. \right.
\end{aligned}$$

$$\begin{aligned}
& + 464681264d^4 - 1052303520d^3 + 1570727840d^2 - 1390172032d + 552221696)t^3 \\
& - 2(120d^{10} - 4895d^9 + 93758d^8 - 1074277d^7 + 8014432d^6 - 40380396d^5 + 138851282d^4 \\
& - 321810020d^3 + 481706112d^2 - 421213824d + 163678208)t^2 \\
& + (-576d^{10} + 19938d^9 - 310357d^8 + 2885938d^7 - 17897281d^6 + 77838658d^5 \\
& - 241230924d^4 + 525745464d^3 - 768104064d^2 + 675136512d - 269293568)t \\
& + 4(d-4)(2d-7)(3d-8)(7d-24)(2d^6 - 45d^5 + 440d^4 - 2400d^3 + 7663d^2 \\
& - 13416d + 9916)) \\
& + 4S_1(d-4)\left((d-4)(d-2)(3d-8)(16d^5 - 392d^4 + 3733d^3 - 17410d^2 + 39947d - 36170)t^6 \right. \\
& + (24d^9 - 1300d^8 + 24690d^7 - 249483d^6 + 1552630d^5 - 6306395d^4 + 16879494d^3 \\
& - 28802184d^2 + 28423376d - 12335232)t^5 \\
& - 2(36d^9 - 1398d^8 + 21038d^7 - 170071d^6 + 835325d^5 - 2632780d^4 + 5431774d^3 \\
& - 7272136d^2 + 5948248d - 2346816)t^4 \\
& - 2(72d^9 - 4140d^8 + 76608d^7 - 734679d^6 + 4286438d^5 - 16242095d^4 + 40585888d^3 \\
& - 64992352d^2 + 60688024d - 25162304)t^3 \\
& + (240d^9 - 8152d^8 + 122076d^7 - 1068369d^6 + 6055692d^5 - 23106495d^4 + 59338384d^3 \\
& - 98712036d^2 + 96264800d - 41807360)t^2 \\
& + (120d^9 - 6980d^8 + 126510d^7 - 1171107d^6 + 6523462d^5 - 23410323d^4 + 55174090d^3 \\
& - 83395432d^2 + 73915776d - 29360896)t \\
& \left. - 2(2d-7)(3d-8)(7d-24)(2d^6 - 44d^5 + 424d^4 - 2301d^3 + 7367d^2 - 12988d + 9676)\right) \\
& - \frac{(\text{MI201})^2}{4(d-4)^2} \times \left[S_3(d^2 - 7d + 16)^2\right] \\
& + \frac{\text{MI201} \times \text{MI201p}}{4(d-4)^2(t-1)}(d^2 - 7d + 16) \\
& \times \left[S_3\left((d-5)(d-4) - (d^2 - 7d + 16)t\right) - S_1\left(2(d-5)(d-4)\right)\right] \\
& - \frac{(\text{MI201p})^2}{4(d-4)^2(d-2)(t-1)^2} \\
& \times \left[S_1\left(2(d-5)(d-4)(d-2)(d^2 - 7d + 20)t - 2(d-5)(d-4)^3(d-3)\right) \right. \\
& + S_3\left((d-5)(d-3)(d-4)^3 - 2(d-5)(d^3 - 9d^2 + 31d - 36)t(d-4) \right. \\
& \left. \left. + (d-2)(d^2 - 7d + 16)^2t^2\right)\right] \\
& - \frac{\text{MI301}}{16(d-4)^3(d-3)(2d-7)t}
\end{aligned}$$

$$\begin{aligned}
& \times \left[S_3 \left((3d-8)(9d^6 - 358d^5 + 4309d^4 - 24466d^3 + 72896d^2 - 110064d + 66080) \right) \right] \\
& + \frac{\text{MI301p}}{384(d-5)(d-4)^2(d-3)(d-2)(2d-7)(3d-14)(3d-10)(t-1)^4t} \\
& \frac{1}{(t+1)(3td-d-10t+6)}(3d-8) \\
& \times \left[4S_1(d-5)(d-4) \left(-(d-2)(3d-10)(504d^6 - 13635d^5 + 150321d^4 - 867796d^3 \right. \right. \\
& \quad + 2774132d^2 - 4665168d + 3229056)t^6 \\
& \quad + (20160d^8 - 540981d^7 + 6439113d^6 - 44379614d^5 + 193384052d^4 \\
& \quad - 544063128d^3 + 961795520d^2 - 973087872d + 429685632)t^5 \\
& \quad - 2(11700d^8 - 310191d^7 + 3684359d^6 - 25590326d^5 + 113383732d^4 - 326829192d^3 \\
& \quad + 595654144d^2 - 624465984d + 286989312)t^4 \\
& \quad - 2(14688d^8 - 341151d^7 + 3411009d^6 - 19076404d^5 + 64722548d^4 - 134442944d^3 \\
& \quad + 162294832d^2 - 97231104d + 17141184)t^3 \\
& \quad + (14472d^8 - 407187d^7 + 5005133d^6 - 35204948d^5 + 155353288d^4 - 441131248d^3 \\
& \quad + 787549200d^2 - 807657024d + 363577344)t^2 \\
& \quad - (1152d^8 - 42423d^7 + 673815d^6 - 6011238d^5 + 32891740d^4 - 112997480d^3 \\
& \quad + 238155264d^2 - 281853504d + 143604864)t \\
& \quad \left. + 4(10-3d)^2(d-6)(d-3)(2d-7)(d^3 - 14d^2 + 60d - 84) \right) \\
& + S_3 \left(-(10-3d)^2(d-2)(129d^7 - 3212d^6 + 34391d^5 - 205404d^4 + 739512d^3 - 1607360d^2 \right. \\
& \quad + 1961376d - 1046016)t^7 \\
& \quad + 4(3d-10)(849d^9 - 30032d^8 + 473927d^7 - 4373749d^6 + 25975613d^5 - 102786064d^4 \\
& \quad + 270537788d^3 - 455956880d^2 + 445763712d - 192286080)t^6 \\
& \quad - (25209d^{10} - 1033338d^9 + 19009043d^8 - 206384706d^7 + 1463111000d^6 - 7071516464d^5 \\
& \quad + 23585007664d^4 - 53575590816d^3 + 79301446912d^2 - 69045440512d + 26844840960)t^5 \\
& \quad + 8(2475d^{10} - 113604d^9 + 2251836d^8 - 25692899d^7 + 188222312d^6 - 929348420d^5 \\
& \quad + 3141614008d^4 - 7194499824d^3 + 10697199936d^2 - 9334245056d + 3632292480)t^4 \\
& \quad + (4077d^{10} - 75930d^9 + 212327d^8 + 6377826d^7 - 84114572d^6 + 512009736d^5 \\
& \quad - 1854381088d^4 + 4202905216d^3 - 5839036544d^2 + 4524404480d - 1481917440)t^3 \\
& \quad - 4(2709d^{10} - 111876d^9 + 2080489d^8 - 22923137d^7 + 165559865d^6 - 818174674d^5 \\
& \quad + 2799104716d^4 - 6540192632d^3 + 9980180672d^2 - 8975227072d + 3609980160)t^2 \\
& \quad + (3285d^{10} - 146778d^9 + 2917887d^8 - 33985466d^7 + 256862728d^6 - 1316665488d^5 \\
& \quad \left. + 4637311856d^4 - 11085869472d^3 + 17223742720d^2 - 15713037312d + 6395443200)t \right)
\end{aligned}$$

$$\begin{aligned}
& - 8(10 - 3d)^2(d - 6)(d - 5)(d - 4)(d - 3)(2d - 7)(d^3 - 14d^2 + 60d - 84) \Big) \Big] \\
& + \frac{\text{MI301pu1}}{256(d - 5)(d - 4)^2(d - 3)(d - 2)(2d - 7)^2(t - 1)^3t(dt^2 - 4t^2 - 2dt + 8t - 7d + 24)} \\
& \times \Big[4S_1(d - 5)(d - 4) \Big(-4(d - 4)(d - 2)(50d^6 - 1311d^5 + 13537d^4 - 71690d^3 \\
& \quad + 207408d^2 - 312720d + 192736)t^5 \\
& \quad + (2552d^8 - 69101d^7 + 822780d^6 - 5613873d^5 + 23949730d^4 - 65265572d^3 \\
& \quad + 110703544d^2 - 106645280d + 44591360)t^4 \\
& \quad - (1072d^8 - 27329d^7 + 330514d^6 - 2440765d^5 + 11734452d^4 - 36715452d^3 \\
& \quad + 71785904d^2 - 79396032d + 37838336)t^3 \\
& \quad - (16496d^8 - 400017d^7 + 4278992d^6 - 26361489d^5 + 102197258d^4 \\
& \quad - 254892476d^3 + 398579064d^2 - 356380672d + 139113984)t^2 \\
& \quad - (10376d^8 - 214955d^7 + 1847346d^6 - 8281675d^5 + 19121020d^4 - 13469588d^3 \\
& \quad - 34656880d^2 + 82573312d - 53170176)t \\
& \quad + 4(d - 3)(2d - 7)(3d - 10)(3d - 8)(7d - 24)(d^3 - 14d^2 + 60d - 84) \Big) \\
& + S_3 \Big(-8(d - 4)(d - 2)(3d - 8)(3d^7 - 119d^6 + 1743d^5 - 13193d^4 + 57458d^3 - 146044d^2 \\
& \quad + 201960d - 117560)t^6 \\
& \quad + (d - 3)(1749d^9 - 61760d^8 + 958255d^7 - 8593272d^6 + 49142988d^5 - 185948688d^4 \\
& \quad + 465510048d^3 - 743169984d^2 + 686097664d - 278865920)t^5 \\
& \quad - 4(1425d^{10} - 53383d^9 + 900152d^8 - 8990014d^7 + 58847091d^6 - 263613479d^5 \\
& \quad + 817847588d^4 - 1733966660d^3 + 2402720288d^2 - 1963651008d + 718318080)t^4 \\
& \quad - 2(525d^{10} - 11849d^9 + 80259d^8 + 263195d^7 - 7904088d^6 + 60076606d^5 - 255495856d^4 \\
& \quad + 676725336d^3 - 1114395648d^2 + 1050515200d - 434903040)t^3 \\
& \quad + 4(2889d^{10} - 112075d^9 + 1935886d^8 - 19637010d^7 + 129674329d^6 - 582890855d^5 \\
& \quad + 1807046696d^4 - 3816289204d^3 + 5255585008d^2 - 4262445824d + 1546163200)t^2 \\
& \quad + (-5475d^{10} + 235357d^9 - 4378649d^8 + 46943563d^7 - 323389276d^6 + 1502599664d^5 \\
& \quad - 4784211872d^4 + 10330949008d^3 - 14504696576d^2 + 11972023296d - 4415692800)t \\
& \quad - 8(d - 5)(d - 4)(d - 3)(2d - 7)(3d - 10)(3d - 8)(7d - 24)(d^3 - 14d^2 + 60d - 84) \Big) \Big] \\
& + \frac{\text{MI302p}}{384(d - 5)(d - 4)^2(d - 3)^2(d - 2)(2d - 7)(3d - 14)(3d - 10)(t - 1)^4t} \\
& \frac{1}{(t + 1)(3td - d - 10t + 6)} \\
& \times \Big[4S_1(d - 5)(d - 4) \Big(-(d - 4)(d - 2)(3d - 10)(504d^6 - 11637d^5 + 113655d^4 - 604084d^3
\end{aligned}$$

$$\begin{aligned}
& + 1847396d^2 - 3079344d + 2177376)t^7 \\
& + 2(11916d^9 - 414225d^8 + 6352830d^7 - 56374909d^6 + 318836394d^5 - 1191362572d^4 \\
& + 2940103576d^3 - 4619041056d^2 + 4189615488d - 1670289024)t^6 \\
& - (103464d^9 - 2938629d^8 + 37503853d^7 - 283016178d^6 + 1394564364d^5 - 4658982648d^4 \\
& + 10555759136d^3 - 15629324544d^2 + 13702223232d - 5408057088)t^5 \\
& - 4(29610d^9 - 782304d^8 + 9109423d^7 - 61230473d^6 + 260959440d^5 - 727545024d^4 \\
& + 1315807272d^3 - 1467083328d^2 + 889375008d - 208577472)t^4 \\
& + (23112d^9 - 886839d^8 + 14132645d^7 - 126227280d^6 + 707027656d^5 - 2599976032d^4 \\
& + 6316590928d^3 - 9818071936d^2 + 8883495168d - 3570219264)t^3 \\
& + 2(5796d^9 - 154869d^8 + 1736686d^7 - 10372501d^6 + 33208662d^5 - 38047564d^4 \\
& - 102311352d^3 + 454295424d^2 - 675620352d + 378190080)t^2 \\
& - (1080d^9 - 39603d^8 + 647143d^7 - 6166938d^6 + 37643332d^5 - 152141288d^4 \\
& + 405964928d^3 - 687895680d^2 + 670167552d - 285405696)t \\
& + 4(10 - 3d)^2(d - 6)(d - 4)(d - 3)(2d - 7)(d^3 - 14d^2 + 60d - 84)) \\
& + S_3 \left(-(10 - 3d)^2(d - 4)(d - 2)(111d^7 - 2300d^6 + 19457d^5 - 85596d^4 + 203904d^3 \right. \\
& \quad - 241472d^2 + 101664d - 384)t^8 + (3d - 10)(5385d^{10} - 226808d^9 + 4182179d^8 \\
& \quad - 44748716d^7 + 309005984d^6 - 1443157120d^5 + 4626129232d^4 - 10065576512d^3 \\
& \quad + 14242561536d^2 - 11844667392d + 4399303680)t^7 \\
& \quad + (-55899d^{11} + 2430714d^{10} - 48230193d^9 + 575086382d^8 - 4570303756d^7 \\
& \quad + 25383400200d^6 - 100436950272d^5 + 282934787520d^4 - 555873116288d^3 \\
& \quad + 725240141568d^2 - 565491947008d + 199649648640)t^6 \\
& \quad + (45999d^{11} - 2250018d^{10} + 48382693d^9 - 609765946d^8 + 5035567328d^7 \\
& \quad - 28727760016d^6 + 115852614736d^5 - 330909888800d^4 + 656973248128d^3 \\
& \quad - 864318028288d^2 + 678672041984d - 241094123520)t^5 \\
& \quad + (20475d^{11} - 620298d^{10} + 8041961d^9 - 56735830d^8 + 219514604d^7 \\
& \quad - 301492744d^6 - 1261549408d^5 + 7829491520d^4 - 19703007104d^3 \\
& \quad + 27190314752d^2 - 19850728448d + 5852774400)t^4 \\
& \quad + (-27279d^{11} + 1276794d^{10} - 26458565d^9 + 323448330d^8 - 2607788888d^7 \\
& \quad + 14621602688d^6 - 58346744400d^5 + 166033462048d^4 - 330601074432d^3 \\
& \quad + 438997027072d^2 - 349978580992d + 126904350720)t^3 \\
& \quad + (-1449d^{11} + 846d^{10} + 1108325d^9 - 25258278d^8 + 286327628d^7 - 2018882504d^6 \\
& \quad + 9546729632d^5 - 31042513536d^4 + 68958355968d^3 - 100505389568d^2
\end{aligned}$$

$$\begin{aligned}
& + 86971736576d - 33976074240)t^2 \\
& + (d-4)(3141d^{10} - 131202d^9 + 2450879d^8 - 26942706d^7 + 192880408d^6 \\
& - 938885584d^5 + 3144719824d^4 - 7150909152d^3 + 10556251264d^2 - 9126496512d \\
& + 3505305600)t \\
& - 8(10-3d)^2(d-6)(d-5)(d-4)^2(d-3)(2d-7)(d^3-14d^2+60d-84)) \Big] \\
& + \frac{\text{MI303p}}{8(d-4)^2(d-3)(d-2)(t-1)^3(t+1)} \\
& \times \Big[\mathcal{S}_3 \Big((d-2)(3d-8)(d^3-10d^2+33d-37)t^4 \\
& + (-13d^5+230d^4-1605d^3+5556d^2-9568d+6560)t^3 \\
& + (17d^5-216d^4+1003d^3-1946d^2+1052d+640)t^2 \\
& + (-23d^5+310d^4-1595d^3+3804d^2-3936d+1120)t \\
& + (2d-7)(8d^4-112d^3+579d^2-1314d+1104) \Big) \\
& + 2\mathcal{S}_1 \Big((d-2)(d^5-7d^4-39d^3+483d^2-1498d+1520)t^3 \\
& + (-5d^6+117d^5-1079d^4+5059d^3-12712d^2+16128d-7968)t^2 \\
& + (-9d^6+249d^5-2367d^4+10759d^3-25280d^2+29124d-12576)t \\
& - (d-4)(3d^5-39d^4+149d^3-57d^2-684d+968) \Big) \Big] \\
& + \frac{\text{MI401}}{16(d-4)^2(2d-7)(3d-8)} \\
& \times \Big[\mathcal{S}_3 \Big(21d^6 - 789d^5 + 9422d^4 - 53864d^3 + 163200d^2 - 253472d + 159232 \Big) \Big] \\
& + \frac{\text{MI402p}}{32(d-4)^2(d-2)(2d-7)(3d-8)(t-1)^3(t+1)} \\
& \times \Big[4\mathcal{S}_1(d-4) \Big(-(d-2)(4d^5+145d^4-2501d^3+13664d^2-31732d+27040)t^3 \\
& - (140d^6-2243d^5+16659d^4-72088d^3+184420d^2-255344d+146176)t^2 \\
& - 2(2d-7)(35d^5-298d^4+632d^3+1196d^2-6008d+5888)t \\
& - 2(2d-7)(d^5-20d^4+176d^3-788d^2+1704d-1408) \Big) \\
& + \mathcal{S}_3 \Big((d-2)(3d^6-475d^5+7498d^4-49896d^3+168688d^2-286624d+194816)t^4 \\
& - 2(39d^7-1375d^6+18274d^5-125446d^4+491184d^3-1109048d^2 \\
& + 1345440d-679168)t^3 \\
& + (3d-8)(57d^6-1575d^5+16796d^4-90904d^3+266832d^2-405520d+250112)t^2 \\
& - 4(2d-7)(15d^6-380d^5+3722d^4-18616d^3+50984d^2-73088d+43008)t \\
& + 4(d-4)(2d-7)(3d^5-46d^4+304d^3-1084d^2+2024d-1536) \Big) \Big]
\end{aligned}$$

$$\begin{aligned}
& + \frac{\text{MI403p}}{64(d-5)(d-4)(d-3)(d-2)(2d-7)(t-1)^3(-10t+d(3t-1)+6)} \\
& \times \left[S_1 \left(4(d-5)(d-4)(d-2)^2(3d-10)(37d^2-309d+626)t^4 \right. \right. \\
& \quad - 8(d-5)(d-4)(d-2)(3d-10)(40d^3-495d^2+1997d-2646)t^3 \\
& \quad + 8(d-5)(347d^6-6556d^5+51757d^4-218326d^3+518564d^2-657064d+346720)t^2 \\
& \quad - 8(d-5)(104d^6-2031d^5+16285d^4-69386d^3+167380d^2-218536d+121184)t \\
& \quad \left. - 4(d-6)(d-5)(d-4)(d-2)(37d^3-365d^2+1070d-872) \right) \\
& + S_3 \left(-(d-2)^2(3d-10)(d^5-44d^4+527d^3-2732d^2+6624d-6224)t^5 \right. \\
& \quad + (d-2)(3d-10)(27d^6-790d^5+9269d^4-56262d^3+187692d^2-327848d \\
& \quad + 234880)t^4 \\
& \quad - 2(3d-10)(31d^7-950d^6+12125d^5-83610d^4+337148d^3-796432d^2 \\
& \quad + 1021712d-549440)t^3 \\
& \quad + 2(67d^8-2284d^7+33437d^6-274288d^5+1381244d^4-4383096d^3 \\
& \quad + 8580512d^2-9494560d+4553600)t^2 \\
& \quad + (-19d^8+614d^7-8801d^6+72650d^5-379420d^4+1290968d^3-2797600d^2 \\
& \quad + 3511168d-1933440)t \\
& \quad \left. - (d-6)(d-2)(7d^6-226d^5+2817d^4-17290d^3+55364d^2-87592d+52800) \right) \Big] \\
& + \frac{\text{MI404p}}{8(d-4)^2(d-3)(d-2)(2d-7)(t-1)^3(3td-d-10t+6)} t^2 \\
& \times \left[4S_1(d-5)(d-4) \left(-(d-4)(d-2)(37d^2-309d+626)t^2 \right. \right. \\
& \quad - 4(4d^4-42d^3+108d^2+71d-374)t \\
& \quad \left. + (d-2)(37d^3-365d^2+1070d-872) \right) \\
& + S_3 \left((d-4)(d-2)(d^5-44d^4+527d^3-2732d^2+6624d-6224)t^3 \right. \\
& \quad + (5d^7-140d^6+1255d^5-3688d^4-8584d^3+83112d^2-198272d+163392)t^2 \\
& \quad + (-13d^7+430d^6-5323d^5+32858d^4-108592d^3+183032d^2-120048d-8000)t \\
& \quad \left. + (d-2)(7d^6-226d^5+2817d^4-17290d^3+55364d^2-87592d+52800) \right) \Big] \\
& + \frac{\text{MI407p}}{8(d-5)(d-4)(d-3)(d-2)(3d-8)(t-1)^3} \times \\
& \left[8S_1(d-5) \left(-(d-5)(d-4)(d-2)(3d-10)(3d-8)t^3 \right. \right. \\
& \quad + (d-4)(d^5-13d^4+42d^3+46d^2-424d+528)t^2 \\
& \quad \left. + (6d^6-167d^5+1653d^4-7988d^3+20388d^2-26312d+13440)t \right)
\end{aligned}$$

$$\begin{aligned}
& + (d-4)(d^5 - 7d^4 - 40d^3 + 450d^2 - 1272d + 1168) \\
& + S_3 \left(6d^7 - 203d^6 + 2774d^5 - 20145d^4 + 84744d^3 - 207740d^2 + 275904d - 153600 \right. \\
& \quad - (d-2)(3d-10)(3d-8)(d^3 - 12d^2 + 47d - 64)t^4 \\
& \quad - 2(3d^7 - 103d^6 + 1415d^5 - 10273d^4 + 43102d^3 - 105320d^2 + 139456d - 77440)t^3 \\
& \quad + 2(d-2)(9d^6 - 260d^5 + 2955d^4 - 17152d^3 + 54140d^2 - 88592d + 58880)t^2 \\
& \quad \left. - 2(d-2)(9d^6 - 263d^5 + 3011d^4 - 17577d^3 + 55748d^2 - 91608d + 61120)t \right) \\
& + \frac{\text{MI408p}}{4(d-5)(d-4)(d-3)(d-2)(3d-8)(t-1)(t+1)} \\
& \times \left[S_3 \left(-(d-2)(3d-8)(d^3 - 12d^2 + 47d - 64)t^4 \right. \right. \\
& \quad + 8(d-5)(2d^4 - 28d^3 + 144d^2 - 325d + 272)t^3 \\
& \quad - 2(13d^5 - 198d^4 + 1139d^3 - 3018d^2 + 3500d - 1216)t^2 \\
& \quad + 8(d-5)(2d-7)(2d^3 - 14d^2 + 29d - 16)t \\
& \quad \left. - (d-4)(19d^4 - 278d^3 + 1485d^2 - 3462d + 2976) \right) \\
& + S_1 \left(-8(d-5)^2(d-4)(d-2)(3d-8)t^3 \right. \\
& \quad + 8(d-5)(d^5 - 19d^4 + 136d^3 - 456d^2 + 702d - 384)t^2 \\
& \quad + 8(d-5)(2d^5 - 53d^4 + 405d^3 - 1322d^2 + 1908d - 960)t \\
& \quad \left. + 8(d-5)(d^5 - 13d^4 + 54d^3 - 52d^2 - 146d + 256) \right) \\
& + \frac{\text{MI409p}}{16(d-4)(d-2)(2d-7)(3d-8)(t-1)^3(dt^2 - 4t^2 - 2dt + 8t - 7d + 24)} \\
& \times \left[4S_1(d-4) \left(-32d^6 - 218d^5 + 10566d^4 - 89360d^3 + 329976d^2 - 573216d + 383104 \right. \right. \\
& \quad - (d-2)(8d^5 - 147d^4 + 1083d^3 - 3940d^2 + 7060d - 5024)t^4 \\
& \quad + (d-2)(3d-8)(24d^4 - 427d^3 + 2681d^2 - 7074d + 6616)t^3 \\
& \quad + (3d-8)(24d^5 - 419d^4 + 2717d^3 - 8314d^2 + 12060d - 6568)t^2 \\
& \quad \left. - (360d^6 - 8561d^5 + 79833d^4 - 379664d^3 + 979684d^2 - 1307264d + 707072)t \right) \\
& + S_3 \left((d-2)(21d^6 - 399d^5 + 3134d^4 - 12848d^3 + 28576d^2 - 32032d + 13568)t^5 \right. \\
& \quad - 2(d-2)(39d^6 - 673d^5 + 4556d^4 - 14898d^3 + 22580d^2 - 9648d - 6016)t^4 \\
& \quad + 2(3d-8)(19d^6 - 327d^5 + 2082d^4 - 5798d^3 + 5144d^2 + 5592d - 9632)t^3 \\
& \quad - 4(93d^7 - 2621d^6 + 29943d^5 - 183067d^4 + 652884d^3 - 1364764d^2 + 1552016d \\
& \quad \left. - 741504)t^2 \right. \\
& \quad \left. + (609d^7 - 18485d^6 + 226344d^5 - 1477312d^4 + 5605424d^3 - 12432304d^2 \right)
\end{aligned}$$

$$\begin{aligned}
& + 14971904d - 7567360)t \\
& - 2(147d^7 - 4603d^6 + 58212d^5 - 392120d^4 + 1533520d^3 - 3500784d^2 \\
& + 4333824d - 2249216)) \Big] \\
& + \frac{\text{MI410p}}{8(d-4)^2(d-2)(2d-7)(3d-8)(t-1)^2(dt^2 - 4t^2 - 2dt + 8t - 7d + 24)} \\
& \times \Big[4S_1(d-4) \Big((d-4)(d-3)(d-2)(3d-8)(5d-22)t^4 \\
& + (d-2)(24d^5 - 599d^4 + 5303d^3 - 21846d^2 + 42692d - 31904)t^3 \\
& - (48d^6 - 1255d^5 + 12775d^4 - 66022d^3 + 184160d^2 - 263888d + 152192)t^2 \\
& - (24d^6 - 515d^5 + 3275d^4 - 4922d^3 - 21408d^2 + 80800d - 74624)t \\
& + 2(24d^6 - 557d^5 + 4749d^4 - 19318d^3 + 38976d^2 - 34784d + 8320) \Big) \\
& + S_3 \Big(-(d-4)(d-3)(d-2)(3d-8)(d^3 - 20d^2 + 104d - 176)t^5 \\
& + 2(d-2)(24d^6 - 595d^5 + 5945d^4 - 30866d^3 + 88216d^2 - 131856d + 80512)t^4 \\
& - 4(45d^7 - 1158d^6 + 12587d^5 - 74941d^4 + 264056d^3 - 550572d^2 + 628624d \\
& - 302976)t^3 \\
& + 2(135d^7 - 3426d^6 + 37341d^5 - 226400d^4 + 823376d^3 - 1791528d^2 \\
& + 2152128d - 1097216)t^2 \\
& + (-177d^7 + 4477d^6 - 49638d^5 + 311844d^4 - 1191016d^3 + 2741632d^2 \\
& - 3491328d + 1883136)t \\
& + 2(d-4)(21d^6 - 449d^5 + 4302d^4 - 23164d^3 + 71416d^2 - 116160d + 76544) \Big) \Big] \\
& + \frac{\text{MI411p}}{16(d-4)(d-3)(d-2)(2d-7)(3d-8)(t-1)(dt^2 - 4t^2 - 2dt + 8t - 7d + 24)} \\
& \times \Big[S_1 \Big(-4(d-4)^2(d-3)(d-2)(3d-8)(5d-22)t^3 \\
& + 8(d-4)(d-2)(8d^5 - 155d^4 + 1187d^3 - 4530d^2 + 8622d - 6512)t^2 \\
& - 4(d-4)(32d^6 - 951d^5 + 10537d^4 - 58056d^3 + 170612d^2 - 255552d + 153088)t \\
& - 8(d-4)(8d^6 - 15d^5 - 1097d^4 + 10424d^3 - 40020d^2 + 71440d - 48960) \Big) \\
& + S_3 \Big((d-4)(d-3)(d-2)(3d-8)(d^3 - 20d^2 + 104d - 176)t^4 \\
& + (d-2)(21d^6 - 405d^5 + 3306d^4 - 14500d^3 + 35904d^2 - 47584d + 26368)t^3 \\
& - (d-4)(177d^6 - 3853d^5 + 34034d^4 - 157624d^3 + 405240d^2 - 548336d \\
& + 304512)t^2 \\
& + (279d^7 - 7465d^6 + 83720d^5 - 514032d^4 + 1872848d^3 - 4053616d^2 + 4823552d \\
& - 2430976)t \Big) \Big]
\end{aligned}$$

$$\begin{aligned}
& -2(63d^7 - 1723d^6 + 19776d^5 - 124416d^4 + 464784d^3 - 1031536d^2 + 1258240d \\
& - 649728)) \Big] \\
& + \frac{\text{MI501p}}{16(d-3)(d-2)(2d-7)(t-1)^3t(t+1)} \\
& \times \Big[S_1 \Big(4(d-4)(d-2)(2d^3 - 32d^2 + 155d - 234)t^5 \\
& - 4(22d^5 - 538d^4 + 4547d^3 - 17726d^2 + 32648d - 22912)t^4 \\
& + 4(308d^5 - 4361d^4 + 25693d^3 - 79592d^2 + 129232d - 86272)t^3 \\
& + 4(308d^5 - 3967d^4 + 19561d^3 - 45038d^2 + 45452d - 12496)t^2 \\
& - 4(2d-7)(11d^4 - 252d^3 + 1760d^2 - 5004d + 5104)t \\
& + 4(d-4)(2d-7)(d^3 - 14d^2 + 60d - 84) \Big) \\
& + S_3 \Big((d-3)(d-2)(d^3 - 20d^2 + 104d - 176)t^6 \\
& - 2(6d^5 - 151d^4 + 1288d^3 - 5082d^2 + 9532d - 6864)t^5 \\
& + 2(59d^5 - 1096d^4 + 8536d^3 - 33882d^2 + 66784d - 51280)t^4 \\
& - 4(36d^5 - 854d^4 + 7448d^3 - 30851d^2 + 61538d - 47584)t^3 \\
& + (-27d^5 - 101d^4 + 3466d^3 - 18324d^2 + 38392d - 29216)t^2 \\
& + 2(2d-7)(17d^4 - 312d^3 + 1992d^2 - 5424d + 5424)t \\
& - 2(d-4)(2d-7)(d^3 - 14d^2 + 60d - 84) \Big) \Big] \\
& + \frac{\text{MI502p}}{16(d-4)^2(d-3)(d-2)(2d-7)(t-1)t(t+1)} \\
& \times \Big[S_1 \Big(4(d-4)(d-2)(2d-9)(8d^3 - 123d^2 + 583d - 870)t^3 \\
& - 8(d-4)(2d-9)(52d^4 - 546d^3 + 2363d^2 - 4971d + 4074)t^2 \\
& - 4(d-4)(2d-9)(104d^4 - 915d^3 + 2687d^2 - 2654d - 24)t \\
& + 16(d-4)(2d-9)(2d-7)(d^3 - 14d^2 + 60d - 84) \Big) \\
& + S_3 \Big(3(d-3)(d-2)(2d-9)(d^3 - 20d^2 + 104d - 176)t^4 \\
& - (2d-9)(41d^5 - 785d^4 + 6198d^3 - 24804d^2 + 49192d - 37888)t^3 \\
& + (2d-9)(57d^5 - 1385d^4 + 12250d^3 - 51224d^2 + 102800d - 79712)t^2 \\
& - (2d-9)(3d^5 - 331d^4 + 3818d^3 - 17188d^2 + 34600d - 26176)t \\
& - 8(d-4)(2d-9)(2d-7)(d^3 - 14d^2 + 60d - 84) \Big) \Big] \\
& + \frac{\text{MI601}}{32(2d-7)} \\
& \times \Big[S_3 t^2 \Big(d^3 - 20d^2 + 104d - 176 \Big) \Big]
\end{aligned}$$

$$\begin{aligned}
& + \frac{\text{MI601p}}{32(2d-7)} \\
& \times \left[\mathcal{S}_1 \left(4(d-4)(3d-20) - 4(d-4)(5d-22)t \right) \right. \\
& + \mathcal{S}_3 \left(d^3 - 20d^2 + 100d + (d^3 - 20d^2 + 104d - 176)t^2 \right. \\
& \quad \left. \left. - 2(d^3 - 20d^2 + 102d - 168)t - 160 \right) \right]. \tag{39}
\end{aligned}$$

B. Definition of the master integrals

The two-loop master integrals are defined as

$$\text{MI} = \int \frac{d^d \ell_1}{i\pi^{d/2}} \frac{d^d \ell_2}{i\pi^{d/2}} \frac{1}{\prod_{j=1}^{15} \mathcal{P}_j^{a_j}}, \tag{40}$$

where the propagators are given by

$$\begin{aligned}
\mathcal{P}_1 &= \ell_1^2, & \mathcal{P}_9 &= (p_2 - q_1 + \ell_1 + \ell_2)^2, \\
\mathcal{P}_2 &= \ell_2^2, & \mathcal{P}_{10} &= \ell_2^2 - m_t^2, \\
\mathcal{P}_3 &= (p_2 - \ell_1)^2, & \mathcal{P}_{11} &= (-p_1 + \ell_1 + \ell_2)^2 - m_t^2, \\
\mathcal{P}_4 &= (q_1 + \ell_2)^2 - m_t^2, & \mathcal{P}_{12} &= (q_2 - p_1 + \ell_1)^2, \\
\mathcal{P}_5 &= (\ell_1 + \ell_2)^2, & \mathcal{P}_{13} &= (p_2 + \ell_1)^2, \\
\mathcal{P}_6 &= (p_1 - q_2 + \ell_1 + \ell_2)^2 - m_t^2, & \mathcal{P}_{14} &= (q_1 + \ell_1)^2 - m_t^2, \\
\mathcal{P}_7 &= (-p_1 + \ell_1)^2, & \mathcal{P}_{15} &= (\ell_1 - \ell_2)^2 - m_t^2, \\
\mathcal{P}_8 &= (q_2 + \ell_2)^2, & &
\end{aligned} \tag{41}$$

with external momenta such that $p_1 + p_2 = q_1 + q_2$, $p_1^2 = p_2^2 = q_2^2 = 0$, $(p_1 - q_2)^2 = t$ and $q_1^2 = m_t^2 = 1$. The powers of the propagators are shown for each master integral in Tab. 2.

In addition, the following one-loop master integrals appear:

$$\text{MI101p} = \int \frac{d^d \ell_1}{i\pi^{d/2}} \frac{1}{\ell_1^2 - m_t^2} \tag{42}$$

$$\text{MI201} = \int \frac{d^d \ell_1}{i\pi^{d/2}} \frac{1}{(\ell_1 + q_2 - p_1)^2 \ell_1^2} \tag{43}$$

$$\text{MI201p} = \int \frac{d^d \ell_1}{i\pi^{d/2}} \frac{1}{(\ell_1 + q_2 - p_1)^2 (\ell_1^2 - m_t^2)}. \tag{44}$$

	a_1	a_2	a_3	a_4	a_5	a_6	a_7	a_8	a_9	a_{10}	a_{11}	a_{12}	a_{13}	a_{14}	a_{15}
MI301	0	0	0	0	1	0	1	1	0	0	0	0	0	0	0
MI301p	1	0	1	1	1	0	0	0	0	0	0	0	0	0	0
MI301pu1	1	0	0	1	1	0	0	0	0	0	0	0	0	0	0
MI302p	0	0	2	1	1	0	0	0	0	0	0	0	0	0	0
MI303p	0	0	0	0	0	0	0	0	0	1	0	0	0	1	1
MI401	0	1	0	0	1	0	1	0	1	0	0	0	0	0	0
MI402p	0	1	1	0	1	1	0	0	0	0	0	0	0	0	0
MI403p	1	1	0	1	0	1	0	0	0	0	0	0	0	0	0
MI404p	1	2	0	1	0	1	0	0	0	0	0	0	0	0	0
MI406t	1	0	0	0	0	0	0	0	0	1	1	1	0	0	0
MI407p	0	0	0	0	0	0	0	0	0	1	0	0	1	1	1
MI407t	2	0	0	0	0	0	0	0	0	1	1	1	0	0	0
MI408p	0	0	0	0	0	0	0	0	0	1	0	0	2	1	1
MI409p	1	0	0	1	1	1	0	0	0	0	0	0	0	0	0
MI410p	1	0	0	1	2	1	0	0	0	0	0	0	0	0	0
MI411p	2	0	0	1	1	1	0	0	0	0	0	0	0	0	0
MI501p	0	1	1	1	1	1	0	0	0	0	0	0	0	0	0
MI502p	0	2	1	1	1	1	0	0	0	0	0	0	0	0	0
MI601	1	1	0	0	1	0	1	1	1	0	0	0	0	0	0
MI601p	1	1	1	1	1	1	0	0	0	0	0	0	0	0	0

Table 2: Two-loop master integrals

References

- [1] R. Dalitz and G. R. Goldstein, “*The Decay and polarization properties of the top quark*”, Phys.Rev. D45, 1531 (1992).
- [2] R. Dalitz and G. R. Goldstein, “*Analysis of top-antitop production and dilepton decay events and the top quark mass*”, Phys.Lett. B287, 225 (1992).
- [3] K. Kondo, T. Chikamatsu and S. Kim, “*Dynamical likelihood method for reconstruction of events with missing momentum. 3: Analysis of a CDF high $p(T)$ $e\mu$ event as t anti- t production*”, J.Phys.Soc.Jap. 62, 1177 (1993).
- [4] D0 Collaboration, V. Abazov et al., “*A precision measurement of the mass of the top quark*”, Nature 429, 638 (2004), hep-ex/0406031.
- [5] P. Kant, O. Kind, T. Kintscher, T. Lohse, T. Martini et al., “*HATHOR for single top-quark production: Updated predictions and uncertainty estimates for single top-quark production in hadronic collisions*”, arxiv:1406.4403.
- [6] G. Bordes and B. van Eijk, “*Calculating QCD Corrections to Single Top Production in Hadronic Interactions*”, Nucl. Phys. B435, 23 (1995).
- [7] M. C. Smith and S. Willenbrock, “*QCD and Yukawa corrections to single top quark production via $q\bar{q} \rightarrow t\bar{b}$* ”, Phys.Rev. D54, 6696 (1996), hep-ph/9604223.
- [8] T. Stelzer, Z. Sullivan and S. Willenbrock, “*Single Top Quark Production via W-Gluon Fusion at Next-To-Leading Order*”, Phys. Rev. D56, 5919 (1997), hep-ph/9705398.

- [9] T. Stelzer, Z. Sullivan and S. Willenbrock, “*Single Top Quark Production at Hadron Colliders*”, Phys. Rev. D58, 094021 (1998), hep-ph/9807340.
- [10] B. Harris, E. Laenen, L. Phaf, Z. Sullivan and S. Weinzierl, “*The Fully Differential Single Top Quark Cross-Section in Next to Leading Order QCD*”, Phys. Rev. D66, 054024 (2002), hep-ph/0207055.
- [11] Z. Sullivan, “*Understanding Single-Top-Quark Production and Jets at Hadron Colliders*”, Phys. Rev. D70, 114012 (2004), hep-ph/0408049.
- [12] Z. Sullivan, “*Angular Correlations in Single-Top-Quark and Wjj Production at Next-To-Leading Order*”, Phys. Rev. D72, 094034 (2005), hep-ph/0510224.
- [13] W. Giele, S. Keller and E. Laenen, “*QCD Corrections to W Boson Plus Heavy Quark Production at the Tevatron*”, Phys. Lett. B372, 141 (1996), hep-ph/9511449.
- [14] S. Zhu, “*Next-To-Leading Order QCD Corrections to $bg \rightarrow tW^-$ at the CERN Large Hadron Collider*”, Phys. Lett. B524, 283 (2002).
- [15] M. Brucherseifer, F. Caola and K. Melnikov, “*On the NNLO QCD corrections to single-top production at the LHC*”, arxiv:1404.7116.
- [16] G. 't Hooft and M. Veltman, “*Regularization and Renormalization of Gauge Fields*”, Nucl.Phys. B44, 189 (1972).
- [17] P. Breitenlohner and D. Maison, “*Dimensional Renormalization and the Action Principle*”, Commun.Math.Phys. 52, 11 (1977).
- [18] M. S. Chanowitz, M. Furman and I. Hinchliffe, “*The Axial Current in Dimensional Regularization*”, Nucl.Phys. B159, 225 (1979).
- [19] G. Bonneau, “*Consistency in Dimensional Regularization With γ_5* ”, Phys.Lett. B96, 147 (1980).
- [20] D. Kreimer, “*The $\gamma(5)$ Problem and Anomalies: A Clifford Algebra Approach*”, Phys.Lett. B237, 59 (1990).
- [21] J. Körner, D. Kreimer and K. Schilcher, “*A Practicable $\gamma(5)$ scheme in dimensional regularization*”, Z.Phys. C54, 503 (1992).
- [22] S. Larin, “*The Renormalization of the axial anomaly in dimensional regularization*”, Phys.Lett. B303, 113 (1993), hep-ph/9302240.
- [23] M. Veltman, “*GAMMATRICA*”, Nucl.Phys. B319, 253 (1989).
- [24] O. Tarasov, “*Connection between Feynman integrals having different values of the space-time dimension*”, Phys.Rev. D54, 6479 (1996), hep-th/9606018.
- [25] O. Tarasov, “*Generalized recurrence relations for two loop propagator integrals with arbitrary masses*”, Nucl.Phys. B502, 455 (1997), hep-ph/9703319.
- [26] C. Anastasiou, E. N. Glover and C. Oleari, “*The two loop scalar and tensor pentabox graph with lightlike legs*”, Nucl.Phys. B575, 416 (2000), hep-ph/9912251.
- [27] A. Pak, “*The Toolbox of modern multi-loop calculations: novel analytic and semi-analytic techniques*”, J.Phys.Conf.Ser. 368, 012049 (2012), arxiv:1111.0868.
- [28] F. Tkachov, “*A Theorem on Analytical Calculability of Four Loop Renormalization Group Functions*”, Phys.Lett. B100, 65 (1981).
- [29] K. Chetyrkin and F. Tkachov, “*Integration by Parts: The Algorithm to Calculate beta Functions in 4 Loops*”, Nucl.Phys. B192, 159 (1981).
- [30] S. Laporta, “*High precision calculation of multiloop Feynman integrals by difference equations*”, Int.J.Mod.Phys. A15, 5087 (2000), hep-ph/0102033.
- [31] C. Anastasiou and A. Lazopoulos, “*Automatic integral reduction for higher order perturbative calculations*”, JHEP 0407, 046 (2004), hep-ph/0404258.
- [32] A. Smirnov, “*Algorithm FIRE – Feynman Integral REduction*”, JHEP 0810, 107 (2008),

- arxiv:0807.3243.
- [33] A. Smirnov and V. Smirnov, “*FIRE4, LiteRed and accompanying tools to solve integration by parts relations*”, Comput.Phys.Commun. 184, 2820 (2013), arxiv:1302.5885.
 - [34] C. Studerus, “*Reduze-Feynman Integral Reduction in C++*”, Comput.Phys.Commun. 181, 1293 (2010), arxiv:0912.2546.
 - [35] A. von Manteuffel and C. Studerus, “*Reduze 2 - Distributed Feynman Integral Reduction*”, arxiv:1201.4330.
 - [36] R. Lee, “*Presenting LiteRed: a tool for the Loop InTEgrals REDuction*”, arxiv:1212.2685.
 - [37] P. Marquard and D. Seidel, unpublished.
 - [38] J. Gluza, A. Mitov, S. Moch and T. Riemann, “*The QCD form factor of heavy quarks at NNLO*”, JHEP 0907, 001 (2009), arxiv:0905.1137.
 - [39] W. Bernreuther, R. Bonciani, T. Gehrmann, R. Heinesch, T. Leineweber et al., “*Two-loop QCD corrections to the heavy quark form-factors: The Vector contributions*”, Nucl.Phys. B706, 245 (2005), hep-ph/0406046.
 - [40] W. Bernreuther, R. Bonciani, T. Gehrmann, R. Heinesch, T. Leineweber et al., “*Two-loop QCD corrections to the heavy quark form-factors: Axial vector contributions*”, Nucl.Phys. B712, 229 (2005), hep-ph/0412259.
 - [41] ATLAS, CDF, CMS, D0 Collaborations, “*First combination of Tevatron and LHC measurements of the top-quark mass*”, arxiv:1403.4427.
 - [42] Particle Data Group Collaboration, J. Beringer et al., “*Review of Particle Physics (RPP)*”, Phys.Rev. D86, 010001 (2012).
 - [43] G. Bell, “*Higher order QCD corrections in exclusive charmless B decays*”, arxiv:0705.3133.
 - [44] G. Bell, “*NNLO vertex corrections in charmless hadronic B decays: Imaginary part*”, Nucl.Phys. B795, 1 (2008), arxiv:0705.3127.
 - [45] G. Bell, “*NNLO vertex corrections in charmless hadronic B decays: Real part*”, Nucl.Phys. B822, 172 (2009), arxiv:0902.1915.
 - [46] R. Bonciani and A. Ferroglia, “*Two-Loop QCD Corrections to the Heavy-to-Light Quark Decay*”, JHEP 0811, 065 (2008), arxiv:0809.4687.
 - [47] M. Beneke, T. Huber and X.-Q. Li, “*Two-loop QCD correction to differential semi-leptonic $b \rightarrow u$ decays in the shape-function region*”, Nucl.Phys. B811, 77 (2009), arxiv:0810.1230.
 - [48] H. Asatrian, C. Greub and B. Pecjak, “*NNLO corrections to $\bar{B} \rightarrow X_u \ell \bar{\nu}$ in the shape-function region*”, Phys.Rev. D78, 114028 (2008), arxiv:0810.0987.
 - [49] T. Huber, “*On a two-loop crossed six-line master integral with two massive lines*”, JHEP 0903, 024 (2009), arxiv:0901.2133.
 - [50] R. Bonciani, P. Mastrolia and E. Remiddi, “*Master integrals for the two loop QCD virtual corrections to the forward backward asymmetry*”, Nucl.Phys. B690, 138 (2004), hep-ph/0311145.
 - [51] S. Borowka, J. Carter and G. Heinrich, “*Numerical Evaluation of Multi-Loop Integrals for Arbitrary Kinematics with SecDec 2.0*”, Comput.Phys.Commun. 184, 396 (2013), arxiv:1204.4152.
 - [52] P. Nogueira, “*Automatic Feynman graph generation*”, J.Comput.Phys. 105, 279 (1993).
 - [53] J. Vermaseren, “*New features of FORM*”, math-ph/0010025.